GEOLOGICAL SURVEY OF FINLAND **DOCUMENTATION PAGE**

Date / Rec. no. Feb 25, 2010 D:no E/782/44/2004

Authors Ilmo Kukkonen, Pekka Heikkinen, Suvi Heinonen, Jukka Laitinen & HIRE Working Group of the Geological Survey of Finland	Type of report Geophysical research report Commissioned by GTK & Pyhäsalmi Mine Oy

Title of report

HIRE Seismic Reflection Survey in the Pyhäsalmi Zn-Cu mining area, central Finland

Abstract

A seismic reflection survey comprising four vibroseis lines (total length of 25.1 km) and two explosion seismic lines (total length 12.5 km) was carried out in the Pyhäsalmi Zn-Cu mining area, in central Finland, in November, 2007. The survey is a part of the project HIRE (*High Resolution Reflection Seismics for Ore Exploration 2007-2010*) of the Geological Survey of Finland (GTK). The Pyhäsalmi survey was done in co-operation with the Pyhäsami Mine Oy.

The Pyhäsalmi area is well known for its massive Zn-Cu sulphide deposits in altered metavolcanic rocks in the thoroughly deformed and folded host rocks of the 1.88-1.93 Ga Savo Belt. The HIRE results show a detailed structure of the uppermost 5 km of crust. The most prominent feature is the bimodal general characteristics of the reflectivity. An E-NE dipping strongly reflective layer was detected at depths exceeding 1-2.5 km. Above this layer the reflectivity is very weak and not simple to correlate with surface geology. Drill hole data from the mine suggest that the strong reflectivity could be attributed to mafic volcanic rocks with interlayers of felsic volcanics and pegmatite dykes at least in the uppermost part of the reflector.

Using large-scale reflection seismic data of the FIRE-1 transect the strongly reflective system can be correlated to a 50 km wide and 10 km deep synform structure of the Savo Belt. Surface geology suggests that the synform and the strongly reflective layer represent mainly mafic volcanic rocks with felsic interlayers as well as metasediments. Considerable shortening has taken place in E-W direction, and several deep, mostly east-dipping (thrust) faults can be identified between Pyhäsalmi and the Archaean-Proterozoic boundary. The Ruotanen and the Mullikkoräme Schist Belts are both located in the immediate vicinity of interpreted deep faults and boundaries of up-thrown blocks.

The Pyhäsalmi deep ore deposit is located at the upper boundary of the strongly reflective layer where the reflectors beneath the deposit seem to form an antiform-like structure. The reflection image of the pear-shaped deep ore body at the depth of 1.1 - 1.5 km is characterized by strong reflectors beneath and on the eastern side of the massive ore. The observed reflectivity is due to impedance contrast between, on one hand, the massive ore and its host rocks (mafic volcanic rocks and interlayers of felsic rocks), and on the other hand, to internal reflection contrasts within the host rocks.

The data is applied for indicating potential targets for further exploration and possible analogues of the Pyhäsalmi deposits.

Keywords: Seismic reflection surveys, massive sulphide deposits, Zn-Cu deposits, Pyhäsalmi, Fennoscandian Shield

Geographical area: Central Finland, Pyhäsalmi

Map sheet: 3321

Other information: This report replaces the draft version dated Aug. 10, 2009

Report serial: Geophysics		Archive code: Q 23/2009/43	
Total pages 49 pages, 8 appendices & digital files	Language English	Price	Confidentiality Not public until Aug. 10, 2010
Unit and section Southern Finland Office, Marine geology and geophysics		Project code HIRE 2321001 HIRE/Pyhäsalmi 1321001	
Signature/name Ilmo Kukkonen		Signature/name	

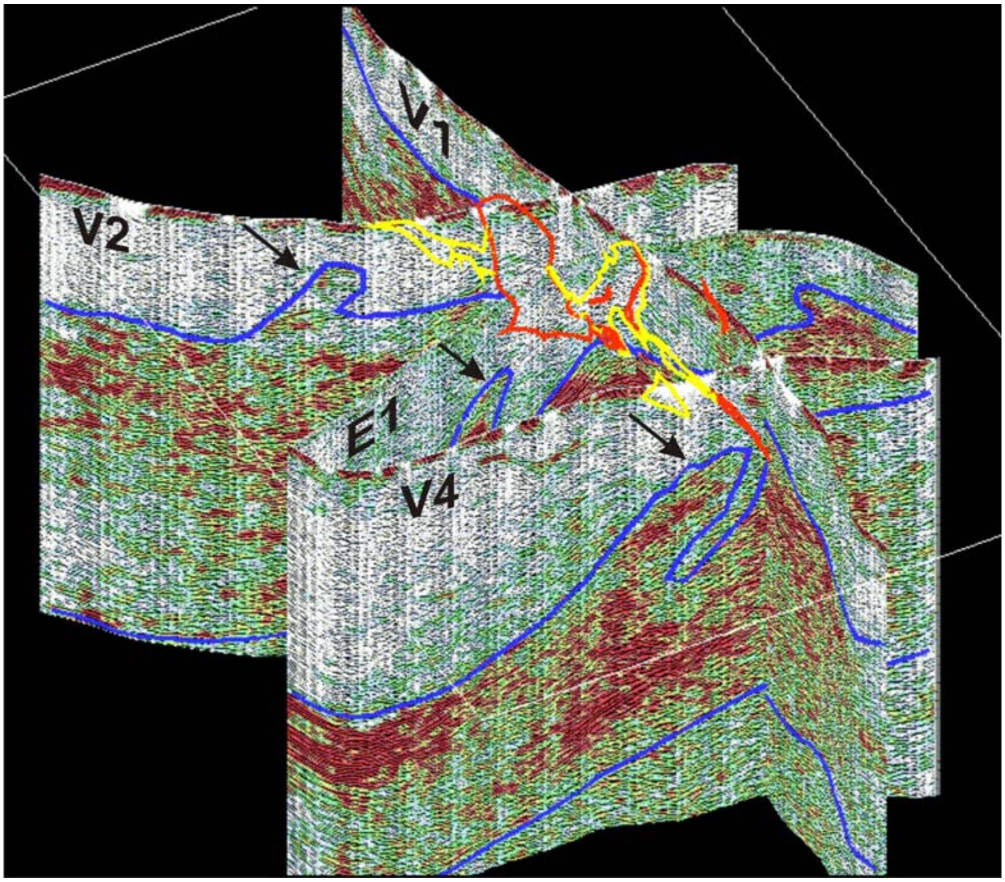

HIRE Seismic Reflection Survey in the Pyhäsalmi Zn-Cu mining area, Central Finland

Ilmo Kukkonen[1], Pekka Heikkinen[2], Suvi Heinonen[2], Jukka Laitinen[1]
& HIRE Working Group of the Geological Survey of Finland

[1]Geological Survey of Finland, P.O.Box 96, FI-02151 Espoo, Finland, e-mail ilmo.kukkonen@gtk.fi
[2]Institute of Seismology, P.O.Box 68, Fi-00014 University of Helsinki, Finland

Report (revised)
Q 23/2009/43
Feb 25, 2010

TABLE OF CONTENTS

Abstract

A seismic reflection survey comprising four vibroseis lines (total length of 25.1 km) and two explosion seismic lines (total length 12.5 km) was carried out in the Pyhäsalmi Zn-Cu mining area, in central Finland, in November, 2008. The survey is a part of the project HIRE (*High Resolution Reflection Seismics for Ore Exploration 2007-2010*) of the Geological Survey of Finland (GTK). The Pyhäsalmi survey was done in co-operation with the Pyhäsami Mine Oy.

The Pyhäsalmi area is well known for its massive Zn-Cu sulphide deposits in altered metavolcanic rocks in the thoroughly deformed and folded host rocks of the 1.88-1.93 Ga Savo Belt. The HIRE results show a detailed structure of the uppermost 5 km of crust. The most prominent feature is the bimodal general characteristics of the reflectivity. An E-NE dipping strongly reflective layer was detected at depths exceeding 1-2.5 km. Above this layer the reflectivity is very weak and not simple to correlate with surface geology. Drill hole data from the mine suggest that the strong reflectivity could be attributed to mafic volcanic rocks with interlayers of felsic volcanics and pegmatite dykes at least in the uppermost parts of the strong reflector.

Using large-scale reflection seismic data of the FIRE-1 transect the strongly reflective system can be correlated to a 50 km wide and 10 km deep synform structure of the Savo Belt. Surface geology suggests that the synform and the strongly reflective layer represent mainly mafic volcanic rocks with felsic interlayers as well as metasediments. Considerable shortening has taken place in E-W direction, and several deep, mostly east-dipping (thrust) faults can be identified between Pyhäsalmi and the Archaean-Proterozoic boundary. The Ruotanen and the Mullikkoräme Schist Belts are both located in the immediate vicinity of interpreted deep faults and boundaries of up-thrown blocks.

The Pyhäsalmi deep ore deposit is located at the upper boundary of the strongly reflective layer where the reflectors beneath the deposit seem to form an antiform-like structure. The reflection image of the pear-shaped deep ore body at the depth of 1.1 - 1.5 km is characterized by strong reflectors beneath and on the eastern side of the massive ore. The observed reflectivity is due to impedance contrast between, on one hand, the massive sulphide ore and its host rocks (mafic volcanic rocks and interlayers of felsic rocks), and on the other hand, to internal reflection contrasts within the host rocks.

Assuming that there originally has been a stratigraphic control of the sulphide deposits at the contact zone between older felsic and younger mafic volcanic rocks, the reflection data can be used to indicate possible targets for exploration. These can be divided in three groups. First, the location of the Pyhäsalmi deep ore deposit at the upper boundary of the strongly reflective layer encourages seeking for analogous sites along the reflector boundary. Second, the presented correlation of surface geology with the HIRE seismic results suggested several potential exploration targets at interpreted mafic/felsic volcanic rock contacts. Third, the structures of the up-thrusted blocks which are associated with altered volcanic rocks on the surface are also potential targets for exploration.

1. Introduction

A seismic reflection survey comprising four vibroseis lines (total length of 25.1 km) and two explosion seismic lines (total length 12.5 km) was carried out in the Pyhäsalmi Zn-Cu mining area, in central Finland, in November, 2007. The survey is a part of the project HIRE (*High Resolution Reflection Seismics for Ore Exploration 2007-2010*) of the Geological Survey of Finland (GTK). The Pyhäsalmi survey was done in co-operation with Pyhäsami Mine Oy.

The general aims of the HIRE project are (1) to introduce reflection surveys as an exploration tool for the Precambrian crystalline bedrock of Finland, (2) to apply 3D visualization and modelling techniques in interpretation, and (3) to improve the structural data base on the most important mineral resource provinces in Finland. The HIRE targets comprise exploration and mining camps in very diverse geological environments. Targets include Cu, Ni, PGE, Zn, and Au deposits, most of them economic, as well as the Finnish site for nuclear waste disposal. The surveys are carried out in co-operation with the companies owning the exploration and mining claims in the survey areas.

The aims of the survey in Pyhäsalmi were to delineate the upper crustal structures of the mining area and its surroundings, and to study the seismic response of the known massive sulphide ore in Pyhäsalmi and its relations to larger scale structures.

The survey was carried out by the Geological Survey of Finland using SFUE Vniigeofizika, Moscow, Russia, as the seismic contractor. The HIRE project is partly funded from the debt conversion agreement between Finland and Russia. The Pyhäsalmi survey was agreed between GTK and Pyhäsalmi Mine Oy based on the offer by GTK dated May 3, 2007.

The survey comprised mainly vibroseismic soundings along roads and two off-road explosion seismic lines. The preparatory works on the explosion lines and drilling of the shooting holes was done in autumn 2007 well before the seismic survey. The topographic survey and seismic data acquisition were carried out during November 16 – 29, 2007.

2. Short geological description of the survey area

The Pyhäsalmi massive Zn-Cu-pyrite deposit is located in the 1.88-1.93 Ga Savo Belt (also known as the Pyhäsalmi Island Arc) characterized by volcanic and metasedimentary rocks (Helovuori, 1979; Kousa et al., 1997). The Savo Belt is located to the west of the eastern Finland Archaean Complex. The Zn-Cu deposits of the Pyhäsalmi area are massive and hosted by altered volcanic rocks, such as sericite schist and cordierite-antophyllite rocks of the 10 km long N-S oriented Ruotanen schist belt of the Pyhäsalmi Volcanic Complex (Fig. 4) (Ekberg and Penttilä, 1986; Mäki and Luukas, 2001). The schist belt is surrounded by Svecofennian granodiorites and granites. The metamorphic grade of the formation is lower-amphibolite facies with peak temperatures and pressures as 600-700 ºC and 5-7 kbar, respectively. Retrograde reactions have taken place at 530 ºC and 2.5 kbar.

The known deposits extended from the surface to about 1.5 km level. The upper part of the deposit mined from 1962 to 2001 was mostly steeply dipping, 10-60 m thick and 105-650 m long in horizontal direction. At about 1 km the sulphide rich zone thins out almost completely in a vertical shear zone, but at depths deeper than 1100 m the deposit thickens and widens again (the new deep ore) and extends to about 1400 m below surface. The deep ore is a pear shaped body a few hundred metres in diameter (Fig. 1).

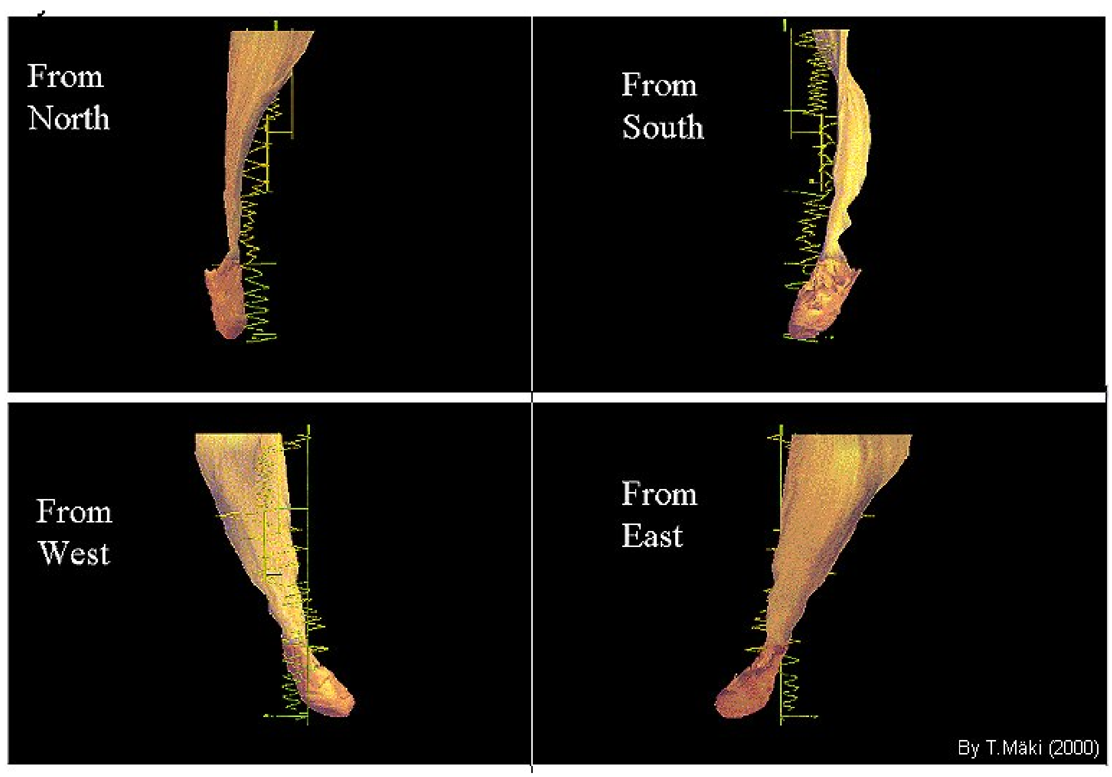

Figure 1. *Views of the Pyhäsalmi deposit (Image: T. Mäki, Pyhäsalmi Mine Oy).*

The ore consist of chalcopyrite (3%), sphalerite (6%), pyrrhotite (2%), pyrite (66%) and about 25% of gangue (barite and carbonate). Original ore reserves were over 54 million tonnes, and at end of 2008 the proven reserves were 13.4 million tonnes with 1.1 % Cu, 2.2 % Zn and 41 % S. (Inmet Mining, 2008).

Genetical models of the Pyhäsalmi deposit describe the original setting as an island arc environment along the Archaean craton margin at about 1.93 Ga. Felsic rhyolitic volcanism was followed by mafic tholeiitic volcanism and sulphide mineralization took place early in a rifted marine environment by extensive hydrothermal circulation near mafic volcanic centres. The originally thin ore layer was thickened and deformed tectonically into its present form (Fig. 2).

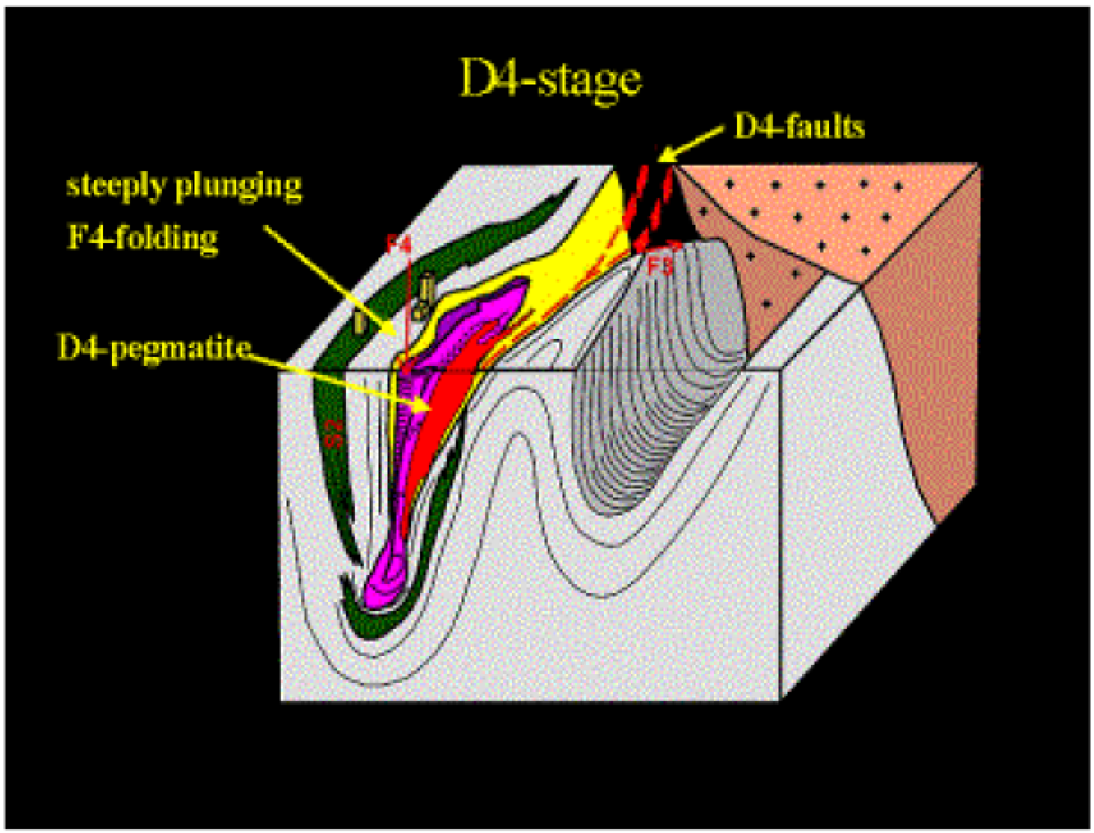

Figure 2. *Structure of the Pyhäsalmi ore deposit and the host rocks (Mäki et al., 2002)*

3. Survey method

The Pyhäsalmi CMP reflection survey consisted of 2D lines located according to the geology, road and terrain conditions. The applied method is the CMP (Common Mid Point) method with symmetrical split-spread geometry, with asymmetric shooting at the end of lines. The number of active channels was 402, and the channel interval was 12.5 m. The maximum offset between source and receivers was 2,502 m in case of symmetrical geometry and at ends of lines in asymmetric geometry up to 5,025 m.

The source point interval was 50 m, and locally, for instance in the vicinity of the Ruotanen schist belt, it was reduced to 25 m. Two source types were applied, i.e., Vibroseis sources and explosions. In Vibroseis surveys, three (minimum two) 15.4 ton Geosvip vibrators were used as a group. The applied force was about 10 ton/vibrator. The sweep was a 16 s linear upsweep with a frequency band of 30-165 Hz, and the total listening time was 22 s. The final correlated signal length is 6 s. The number of sweeps/source point was six. The sweeps were stacked and the stacked data were saved.

In the explosion lines a typical shot size was 125 or 250 g of dynamite. Shot holes were drilled in the Quaternary soil to a depth of 2.5 m, and cased with a plastic tube. Before shooting the holes were filled with water to maximize the transmission of seismic energy to the ground.

Geodetic positioning of the lines was done with GPS (positioning and erecting poles at drilling sites of shooting holes), and immediately before the acquisition with 25 m steel rope (line layout, recording station poles). Horizontal positioning was done with differential GPS to an accuracy of at least ±2 m, and elevations were determined with levelling to an accuracy of at least ± 0.5 m.

The survey parameters are shown in Table 1 (Zamoshnyaya and Sorokina, 2008).

Table 1. Survey parameters.

	Vibroseis	Explosion
Recording	I/O-4	I/O-4
Number of active channels	402	402
Sampling interval, ms	1	1
Record length after correlation, s	6	6
Preliminary gain, dB	24÷36	24÷48
Notch filter, Hz	off	
Noise suppression editor (BURST+DIVERSITY)	on	on
High-pass filter, Hz	off	30
Tape format	SEG-Y	SEG-Y
Medium type	HARD	HARD
Acquisition geometry	Symmetrical split spread	Symmetrical split spread
Stacking fold	varying	varying
Receiver group spacing, m	12.5	12.5
Spacing of source locations, m	25 or 50	50
Spread length, m	5012.5	5012.5
Linear geophone grouping	12 geophones on 12.5 m base	6 geoph. at a point or 3 swamp geoph. at a point
Linear SV-14-150 vibrator grouping	3 on 25 m base	
Sweep frequency limits, Hz	30÷165	
Sweep period, s	16	
Number of vibrations at a source point	6	
Shot hole number at a source point		1
Shot hole depth, m		2.5
Charge weight, g		125 or 250
Ground force	65%	
Control system and vibrator synchronization control	VIB PRO	Shot PRO

4. Data processing

Data processing was done in three main steps. First, on-site processing was done by Vniigeofizika in the field base. The first results were used mainly for quality control. Second, basic processing was continued from the field results in the Moscow office of Vniigeofizika. Third, post stack processing was done by the Institute of Seismology of the University of Helsinki (HY-Seismo), working as a contractor and research partner for GTK.

The on-site and basic processing sequence of data processing is shown in Tables 2-5 (Zamoshnyaya and Sorokina, 2008).

Post stack processing was made by HY-Seismo starting from the NMO stacked sections by Vniigeofizika. The post stack processing included four processing steps:

1) Whole trace amplitude equalization,
2) Stolt migration with depth dependent velocity function,
3) Spectral balancing,
4) Depth conversion.

The purpose of the first step was to eliminate the amplitude variations along the lines caused by changes in surface conditions and possible processing artifacts. The second step improves the migration results as the original migrations were done using the constant velocity of 5000 m/s. As a part of the basic processing, Vniigeofizika performed velocity analysis at every 100th CMP. From the measured values the average Vrms-velocity was estimated and this velocity function was used in Stolt migration. This takes into account the average increase of velocity as a function of traveltime, i.e. depth. The measured stacking velocities as well as the velocity function are shown in Fig. 3. In the upper part (TWT less than 250 ms, corresponding to the depth of about 750 m) the velocity function is above the average value, following the stacking velocities measured on the line V1 between the CMP values 2700-3000. The aim is to have sections and depth estimates as representative as possible close to the present mine.

In the spectra of the migrated traces the amplitudes decrease as a function of frequency, which results correspondingly in decreasing the resolution of the data. This can be improved by spectral balancing, i.e. by increasing the contribution of higher frequencies. Spectral balancing was done multiplying the spectra with a linearly increasing function of the frequency. The applied value of the multiplier was 1.0 at 40 Hz and 2.0 at 160 Hz.

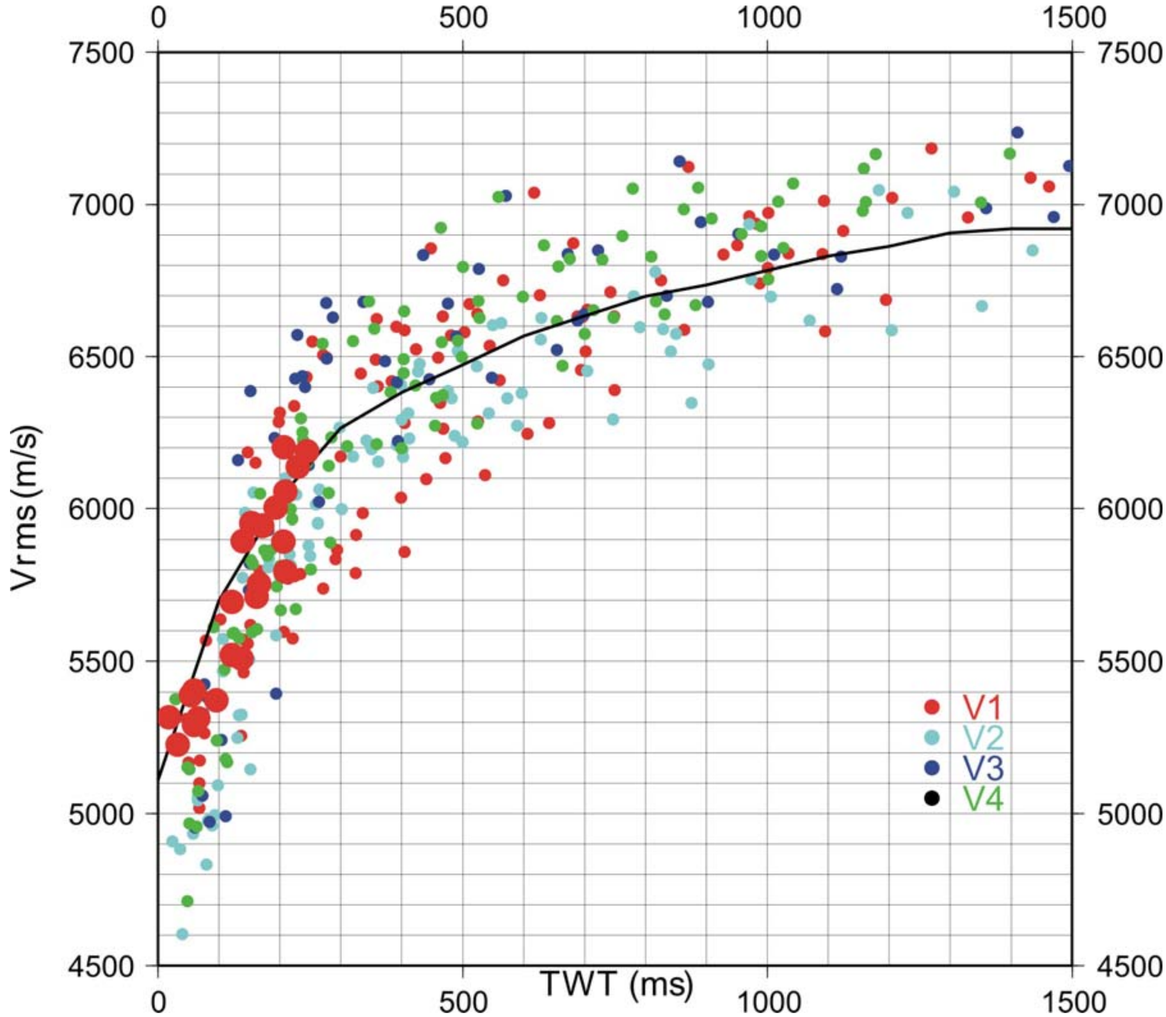

Figure 3. *The measured stacking velocitites (colored dots) and the velocity function used for post stack processing (black line). The color of the dot indicates the line (V1-V4). The large red dots are measured stacking velocities from the line V1 between the CMPs 2700-3000.*

The migrated traces are functions of traveltime and before plotting they have to be converted to functions of depth. The conversion velocity was calculated from the average interval velocities estimated from the average stacking velocity function. The values of the depth conversion velocity are listed in Table 6. Between the listed values linear interpolation was used. The difference between the stacking velocity of Fig. 3 and the depth conversion function is very small, less than 10 m/s. As one can see in Fig. 3, the variation of the velocities is of the order of 4-5 % and similar error can be expected in depth conversion.

Table 2. On-site processing of vibroseis data.

1.	2D geometry application
2.	Band-pass filtering 30-40-140-165 Hz
3.	Spherical divergence compensation
4.	Amplitude equalization, window 300-5000 ms
5.	Spiking deconvolution: noise 0.1 %, OL 80 ms, w 200-2500 ms
6.	Band-pass filtering 30-40-140-165 Hz
7.	Amplitude equalization, window 0-5000 ms
8.	Trace editing
9.	Datum statics correction
10.	1st moveout correction, surgical mute
11.	FK-filtering on seismograms with moveout corrections
12.	Automatic statics correction: calculation window 200-2900 ms, maximum allowable shift 6 ms
13.	2nd moveout correction, surgical mute
14.	Stacking
15.	Amplitude equalization, window 0-6000 ms
16.	Time-variant band-pass filtering: 35-45-140-165 Hz and 30-40-130-160 Hz in windows 0-1500 ms and 1000-6000 ms correspondingly
17.	Noise space filter
18.	Coherence filter
19.	Automatic gain control: 0-800, 600-2500, 2200-4500, 4000-5500, 5000-6000 ms

Table 3. On-site processing of explosion data.

1.	2D geometry application
2.	Band-pass filtering 30-40-200-260 Hz
3.	Spherical divergence compensation
4.	Amplitude equalization, window 300-5000 ms
5.	Predictive deconvolution: noise 0.1 %, OL 100 ms, prediction distance 10 ms, windows 0-2000, 1800-4000 ms
6.	Band-pass filtering 30-40-200-260 Hz
7.	Amplitude equalization, window 0-5000 ms
8.	Trace editing
9.	Datum statics correction
10.	1st moveout correction, surgical mute
11.	FK-filtering on seismograms with moveout corrections
12.	Automatic statics correction: calculation window 200-2900 ms, maximum allowable shift 6 ms
13.	2nd moveout correction, surgical mute
14.	Stacking
15.	Amplitude equalization, window 0-6000 ms
16.	Time-variant band-pass filtering: 40-50-120-220 Hz, 35-45-115-215 Hz, 30-40-110-210 Hz in windows 0-700 ms, 500-2400 ms, 2200-6000 ms correspondingly
17.	Noise space filter
18.	Coherence filter
19.	Automatic gain control: 0-800, 600-2500, 2200-4500, 4000-5500, 5000-6000 ms

Table 4a. Basic processing of vibroseis data.

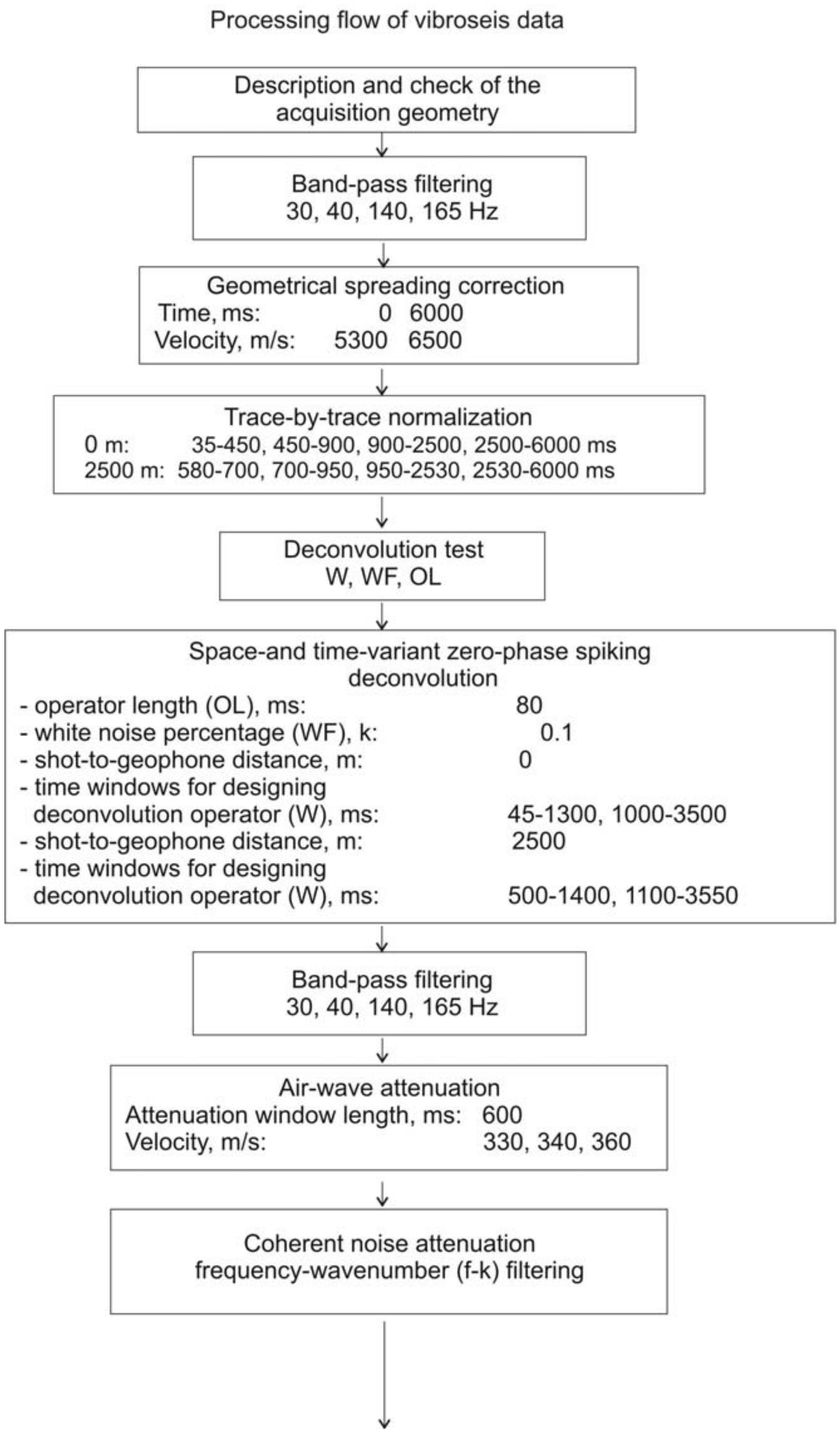

Table 4b. Basic processing of vibroseis data (cont.).

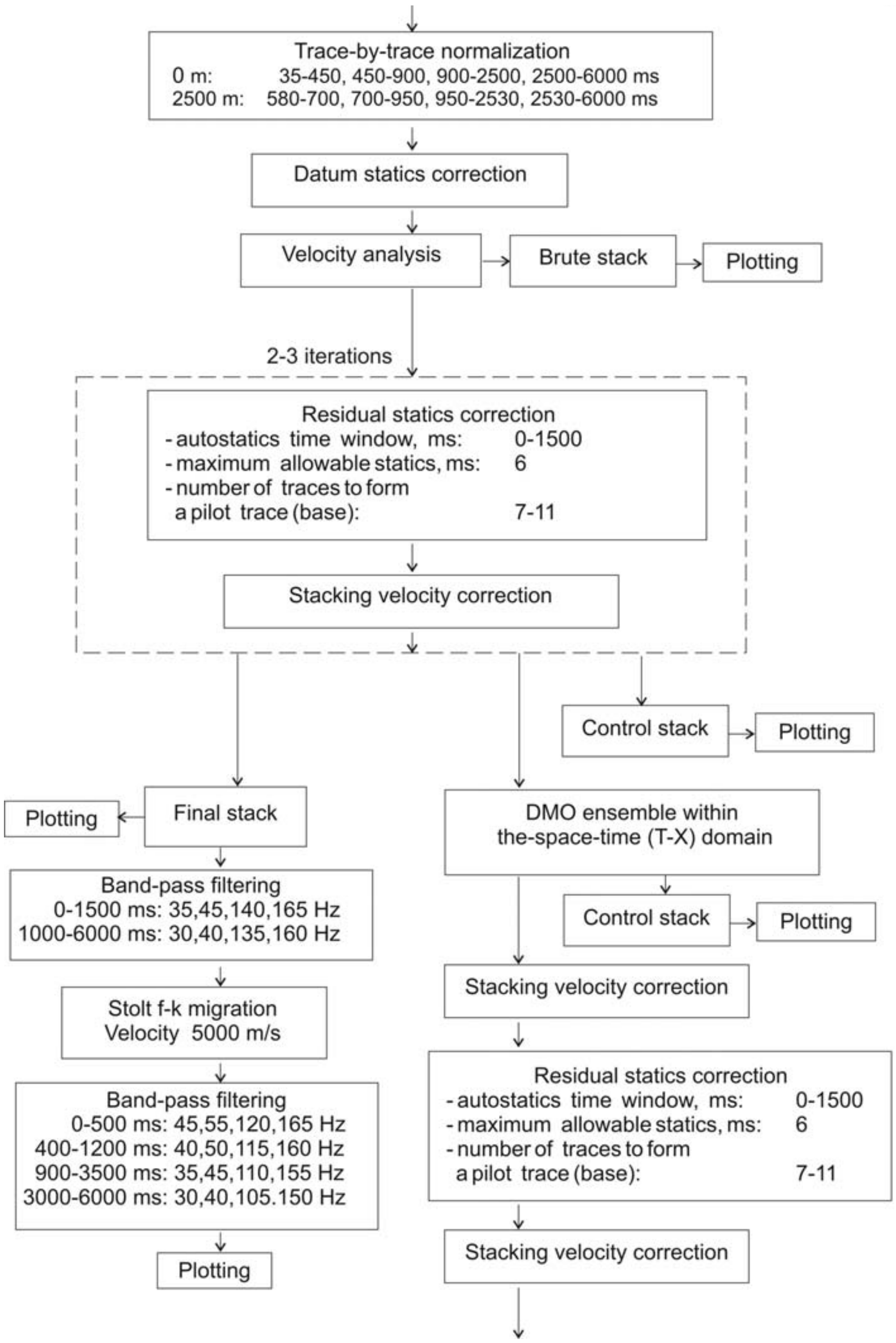

Table 4c. Basic processing of vibroseis data (cont).

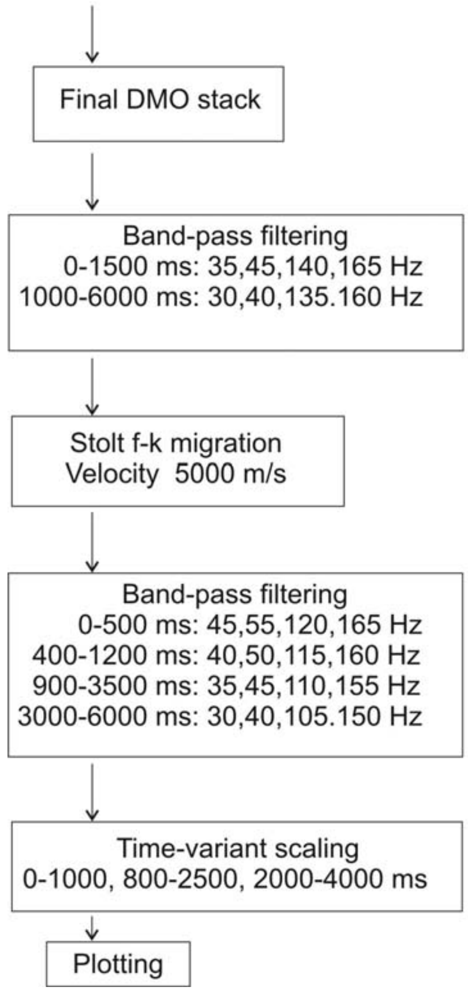

Table 5a. Basic processing of explosion data.

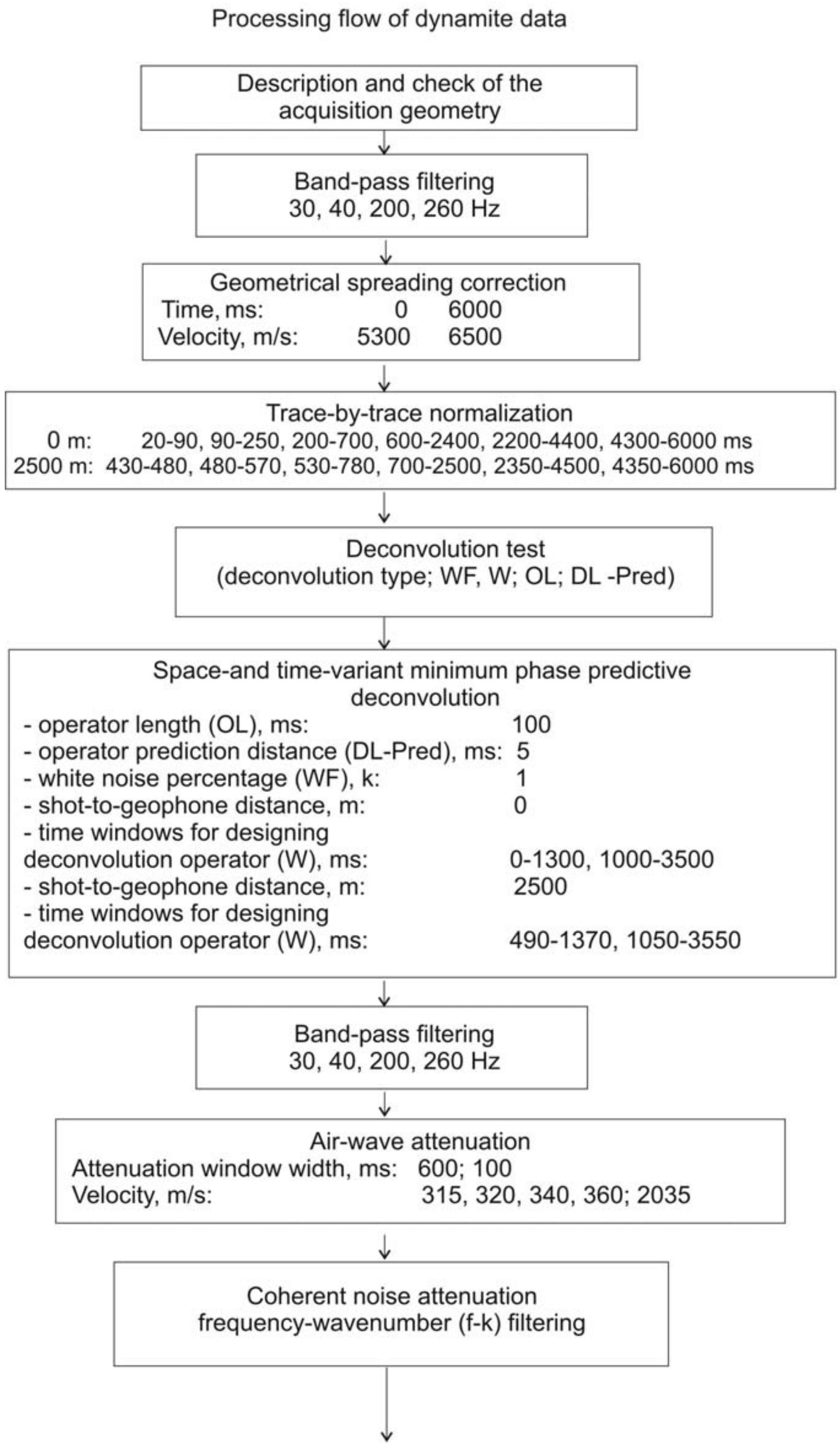

Table 5b. Basic processing of explosion data (cont.).

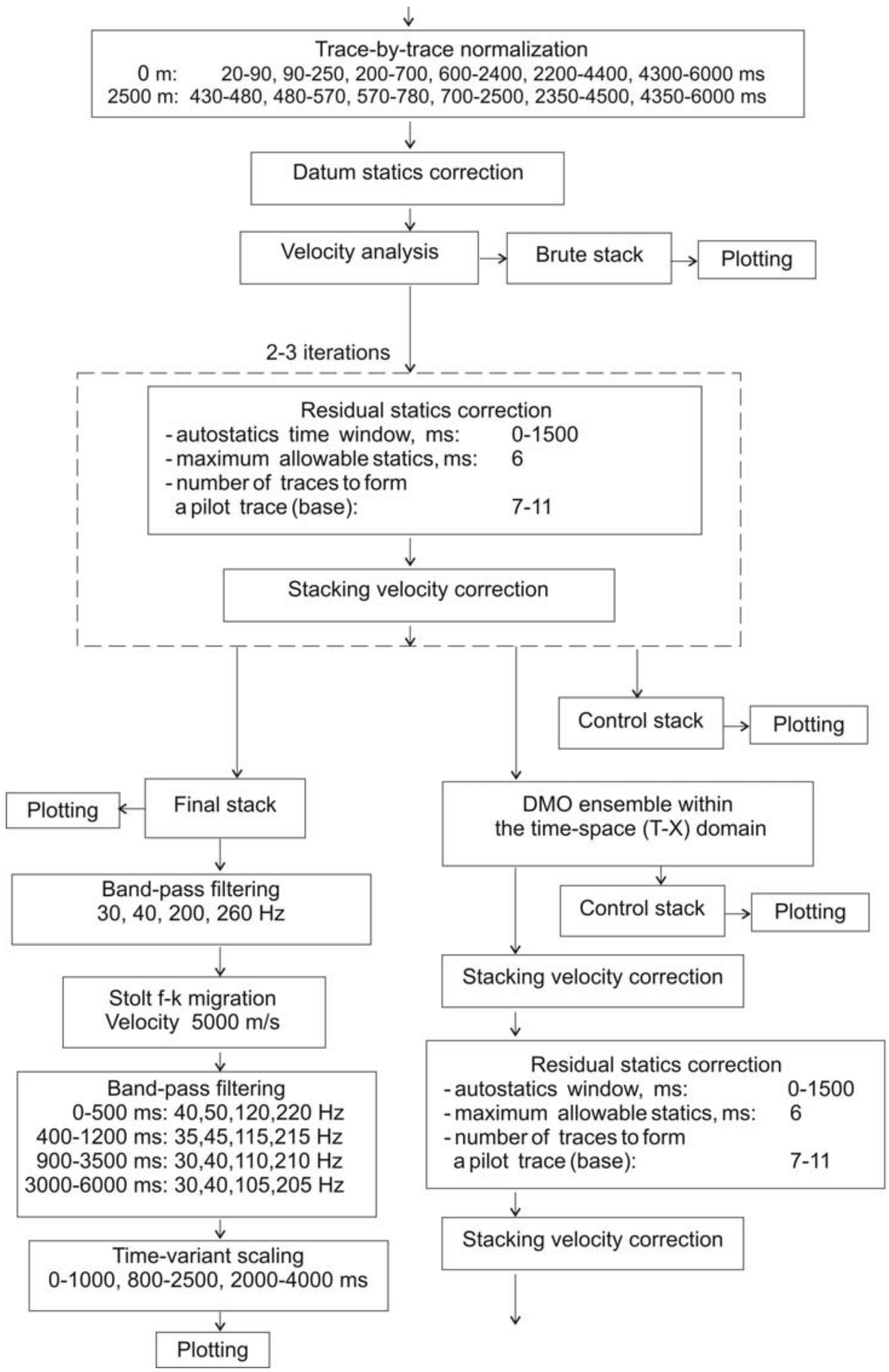

Table 5c. Basic processing of explosion data (cont.).

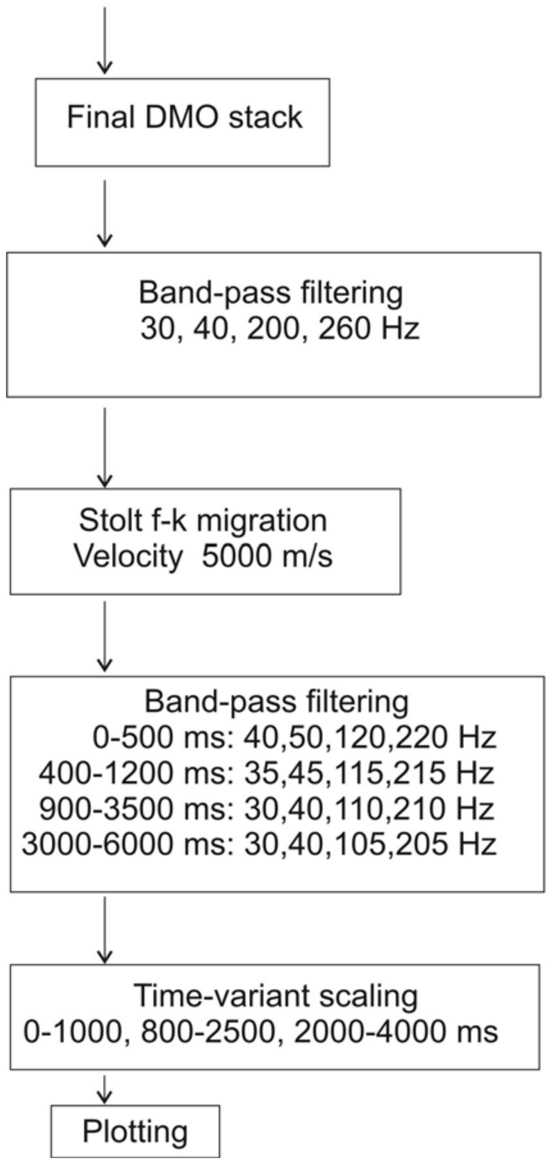

***Table 6. Steps of post-stack processing*.**

Final DMO stack →

Migration (Stolt)

TWT (ms)	V_{rms} (m/s)	TWT (ms)	V_{rms} (m/s)
0	5110	1100	6831
100	5700	1200	6862
200	6035	1300	6906
300	6265	1400	6920
400	6381	1500	6920
500	6472	1600	6931
600	6567	1700	6948
700	6634	1800	6956
800	6699	1900	6961
900	6735	2000	6963
1000	6782		

→

Spectral balancing
Band pass filter

Frequency	Filter amplitude
20.0	0.0
40.0	1.0
160.0	2.0
200.0	2.0
240.0	0.0

→

Depth conversion

Depth (m)	Conversion Vel. (m/s)	Depth	Conversion velocity
0	5110	3384	6769
285	5700	3749	6817
603	6026	4109	6849
938	6251	4480	6892
1274	6368	4835	6906
1615	6459	5181	6908
1966	6553	5535	6919
2317	6620	5896	6937
2674	6684	6251	6945
3024	6721	6604	6951
		6953	6953

→

Plotting

5. Results

5.1. 2D and 3D presentation of the results

The location of the survey lines is shown on a geological map in Fig. 4 and on a magnetic map in the Appendix 2. The map shows two lines for each section, first the receiver station line as it was located in the field, and second, the common mid point (CMP) line. The CMP line indicates the surface projection of average locations of reflection points. For a deep and long section these may differ noticeably if the survey line is curved or crooked. This issue must be taken into account, when locating reflectors in the field. Those very close to surface (less than ca. 200 m) are best located with the shooting line in the terrain, whereas deeper reflectors are best located with the CMP line.

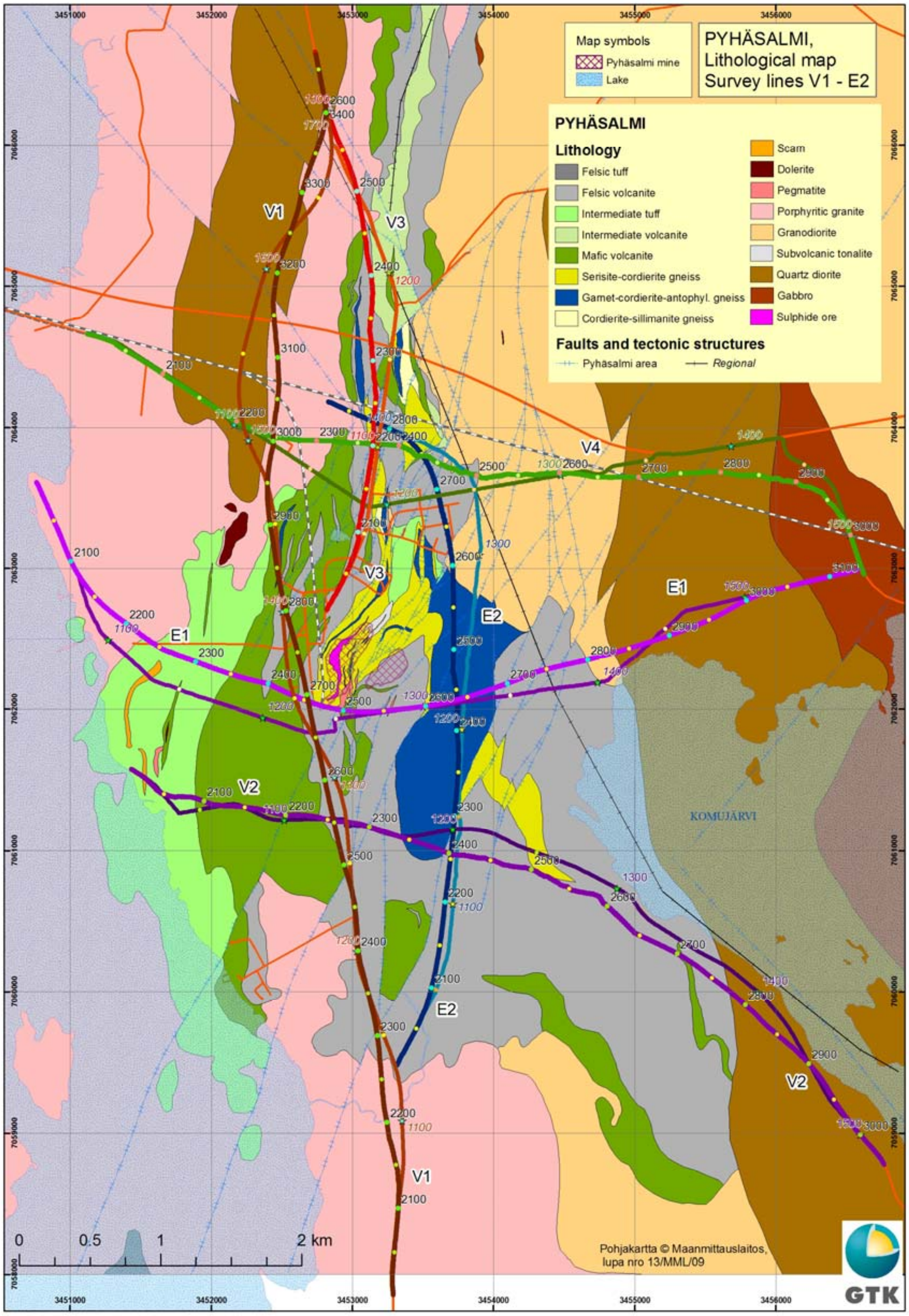

Figure 4. *Survey lines in Pyhäsalmi. Numbers along the lines indicate receiver station pole numbers (italics) and CMP coordinates (normal text).*

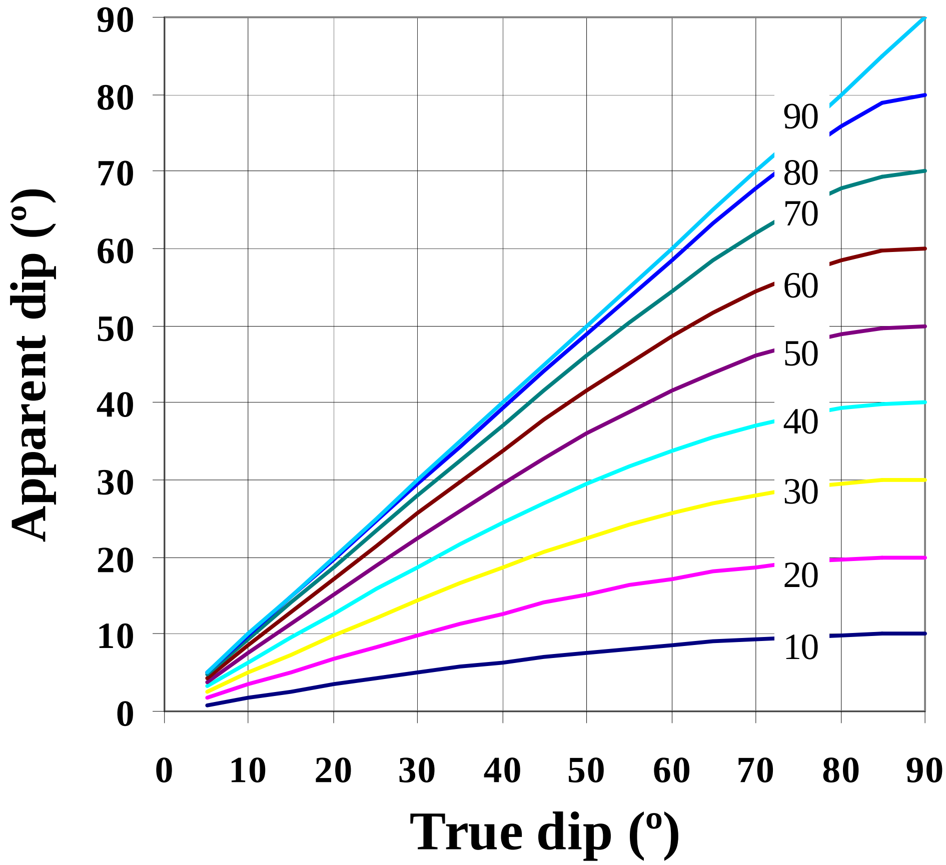

Figure 5. *relations between true and apparent dip angles of planar reflectors. The curve parameter is the angle between the survey line and the strike of the reflector at surface.*

When interpreting 2D seismic sections the effects of the cross dip of reflecting structures must be taken into account. The apparent dip of a planar reflector as seen in the seismic section depends on the true dip and strike of the reflector. If the strike is perpendicular to the line, the apparent dip is equal to the true dip, but the more the strike angle deviates from perpendicular, the smaller becomes the apparent dip angle. The relations between true and apparent dip are shown in a nomogram in Fig. 5. As can be seen in the figure, subvertical structures surveyed at small strike angles are imaged with apparent dip angles significantly smaller than the true dip.

Datum level of the reflection data is 150 m a.s.l. The uppermost layers (Quaternary sediments, weathered bedrock) have lower velocities than the intact crystalline rocks. Velocity and thickness variations of the surface layer generate spatially dependent delays in the arrival times of reflections, and the data must be corrected for these ‘static’ effects. This is done by shifting the signals to a common depth level, which is usually the highest level of topography in the survey area. The datum level is also the level to which the upper boundary of seismic sections (depth 0 m) should be referenced.

Frequency content of the data is very good. Examples of frequency spectra are shown in Figs. 6 and 7. In vibroseis data the applied frequency band of 30-165 Hz is well covered with received data. In the explosion data the achieved spectral content is even wider due to the detonation source and the data is at least 20 dB above noise level in the frequency band applied in data processing (30-260 Hz, Table 5). This predicts good resolution in the final images.

The processed sections show a wealth of reflectors. Reflectors as thin as 10 m vertically and 200-300 m wide horizontally can be distinguished in the sections.

The results of the survey are shown in migrated and depth converted NMO (normal-move-out) sections in Figs. 8-13 and in the appendices. The sections were converted from time sections to depth sections using the velocity function in Table 6. In the figures and appendices the reflectors are displayed as variable area plots of averaged instantaneous amplitude (traces). In addition, the amplitudes were averaged in moving windows (60 m in vertical and 90 m in horizontal directions, respectively) and displayed in dB scale in the background as a color-coded map. Lithological boundaries are given on the top of the 2D sections according to the data base on Precambrian geology (scale 1:200 000) of the GTK.

To obtain three-dimensional visualization of the reflector structures, the seismic sections were input to *SURPAC* 3D visualization and modelling software. The sections were imported into *SURPAC* as images which were draped along vertical ‘curtains’ defined by the CMP coordinates of the lines. Relevant units were interpreted first from the sections in 2D, and the corresponding strings were digitized again in *SURPAC* on the drape surfaces of the sections. As a result, the 3D correlation of the strongly reflective units is presented with the 3D strings.

Only selected examples of the 3D images are shown here (e.g. Figs. 15, 18 and 21). In addition to seismic reflection images, the available maps on bedrock geology and airborne magnetic map were also applied to provide a means to correlate reflectors with bedrock structures. These correlations were used in the interpretations below.

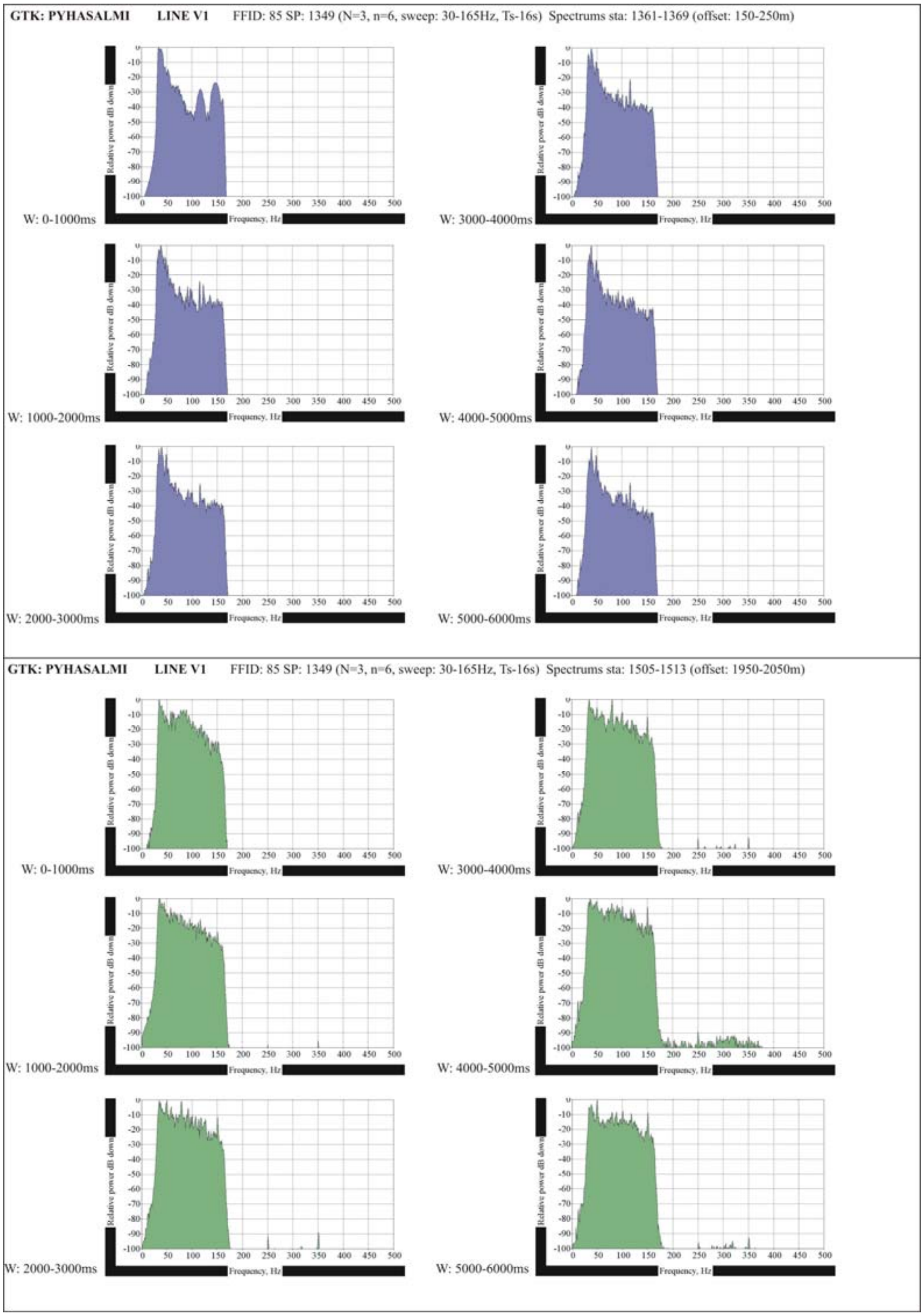

Figure 6. *Frequency spectra of the vibrator field data from V1 with two offsets from the shot point. Upper panels: offset 150-200 m, lower panels: offset 1950-2050 m. (Zamoshnyaya and Sorokina, 2008). The shot point is at CMP 2698 above the deep ore.*

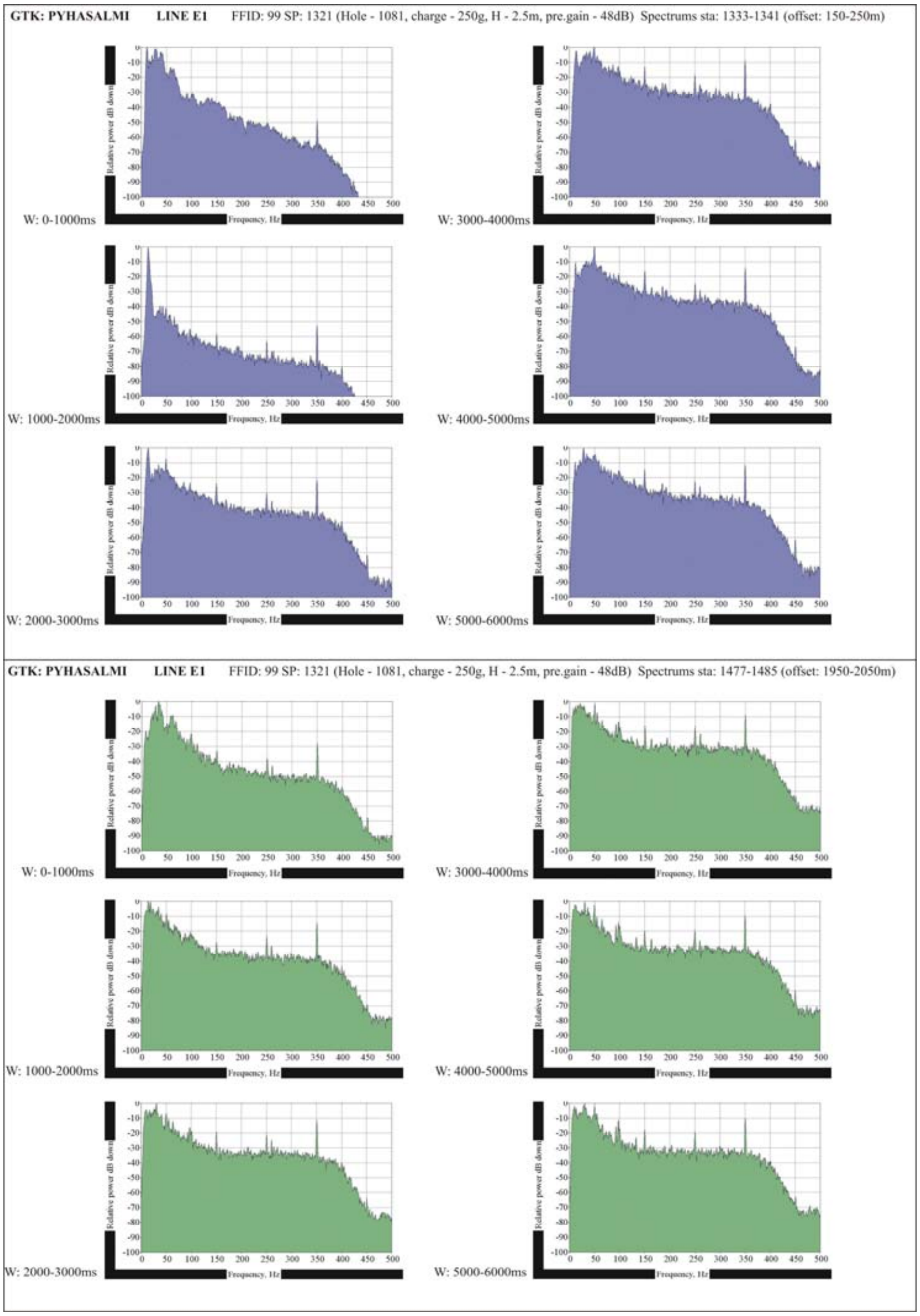

Figure 7. *Frequency spectra of the explosion seismic field data from E1 with two offsets from the shot point. Upper panels: offset 150-200 m, lower panels: offset 1950-2050 m. Shot point location (CMP 2642) is about 1 km to the east of the deep ore (Zamoshnyaya and Sorokina, 2008).*

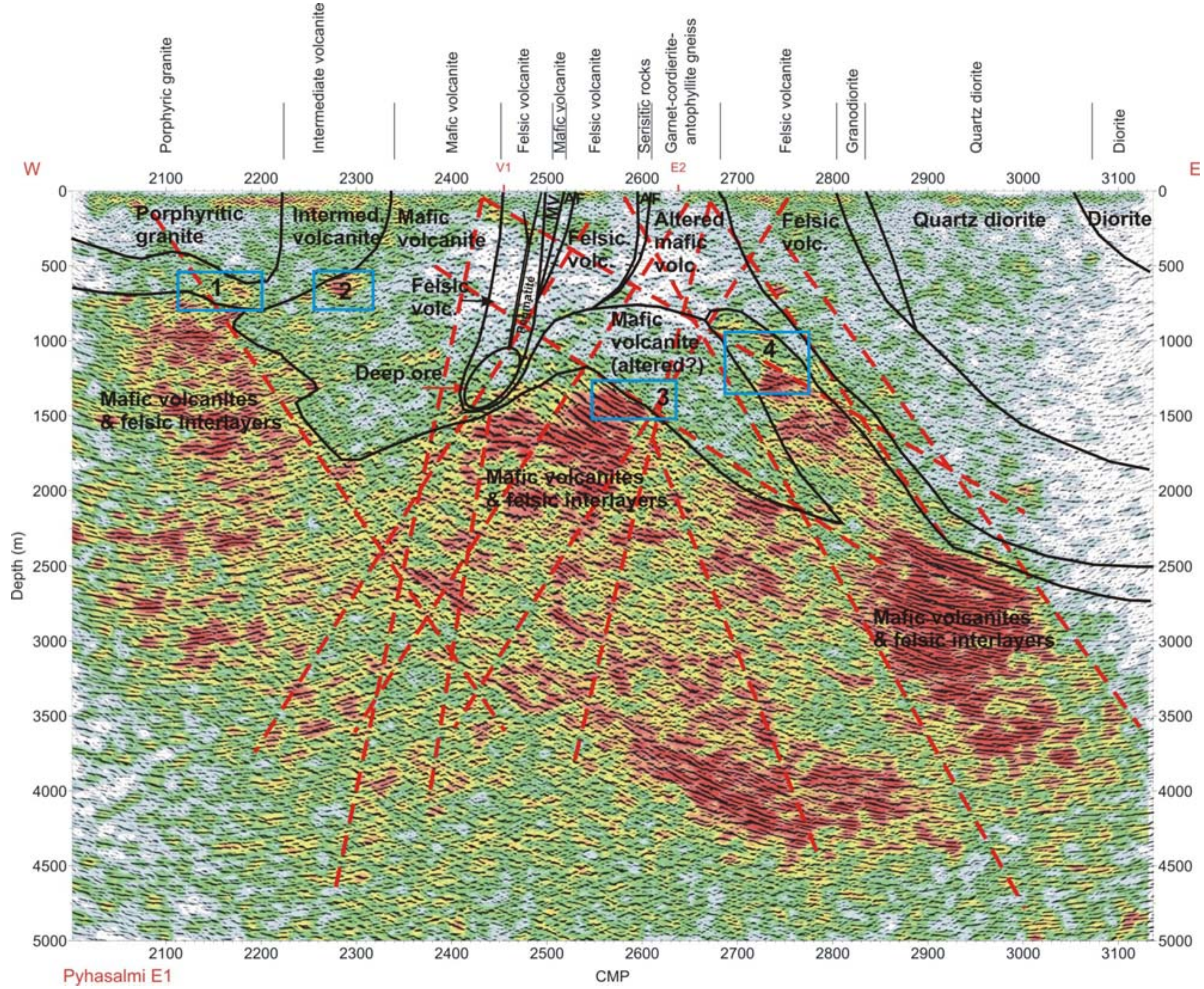

Figure 8. *Migrated NMO section of line E1 and its interpretation. Reflectors with high amplitude are automatically enhanced with red background colour. Geological boundaries at the surface are from the geolocical database of GTK (1:200 000 scale bedrock geology). The boundaries of interpreted geological boundaries are shown with black lines. The red lines indicate interpreted shear and fault zones. FV: felsic volcanic rocks; AF: altered felsic volcanic rocks; MV: mafic volcanic rocks. The blue boxes with numbers indicate suggested exploration targets (Table 7).*

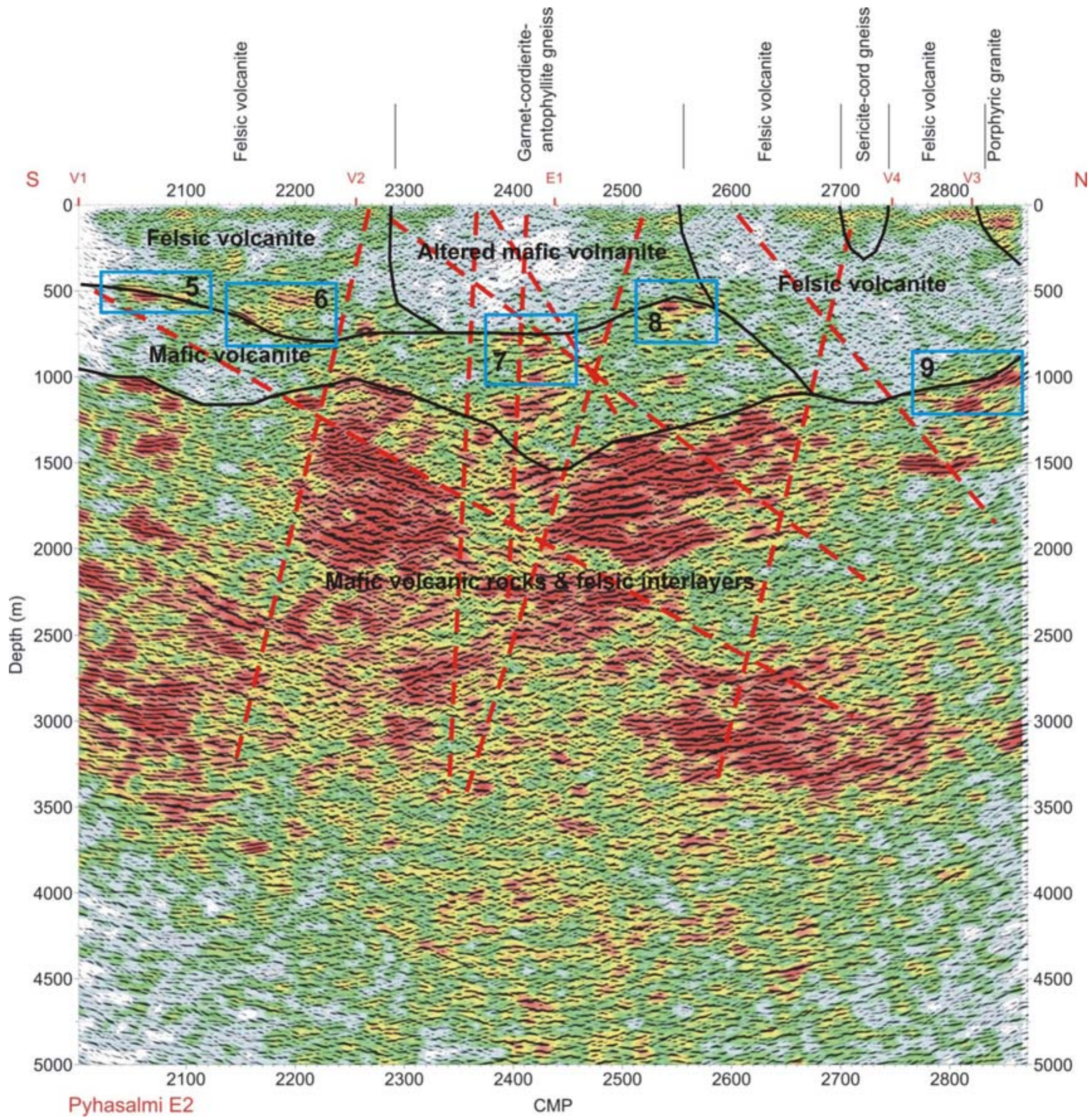

Figure 9. *Migrated NMO section of line E2 and its interpretation. Data representation and geological boundaries as in Fig 7.*

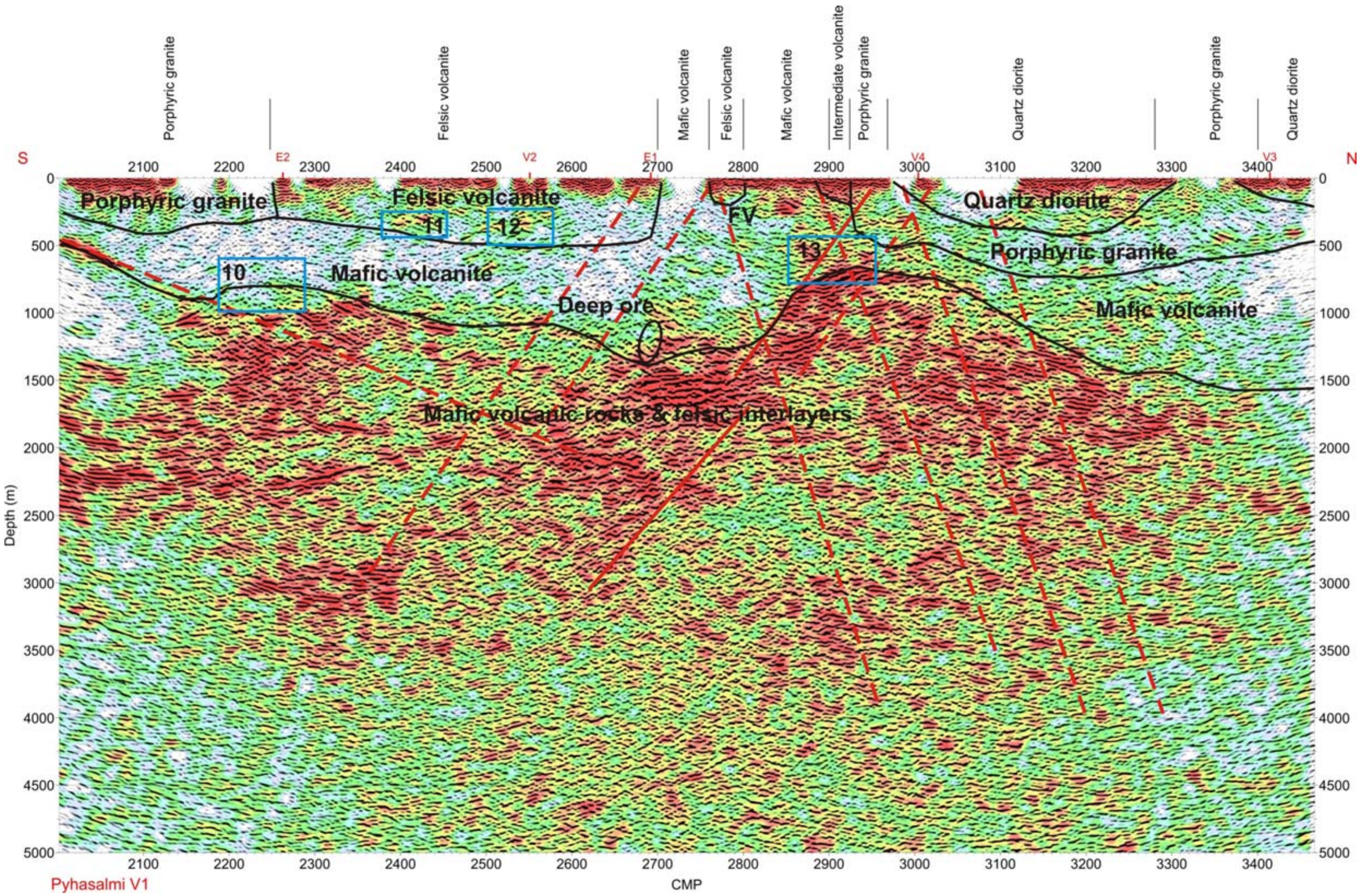

Figure 10. *Migrated NMO section of line V1 and its interpretation. Data representation and geological boundaries as in Fig. 8. FV: felsic volcanic rocks.*

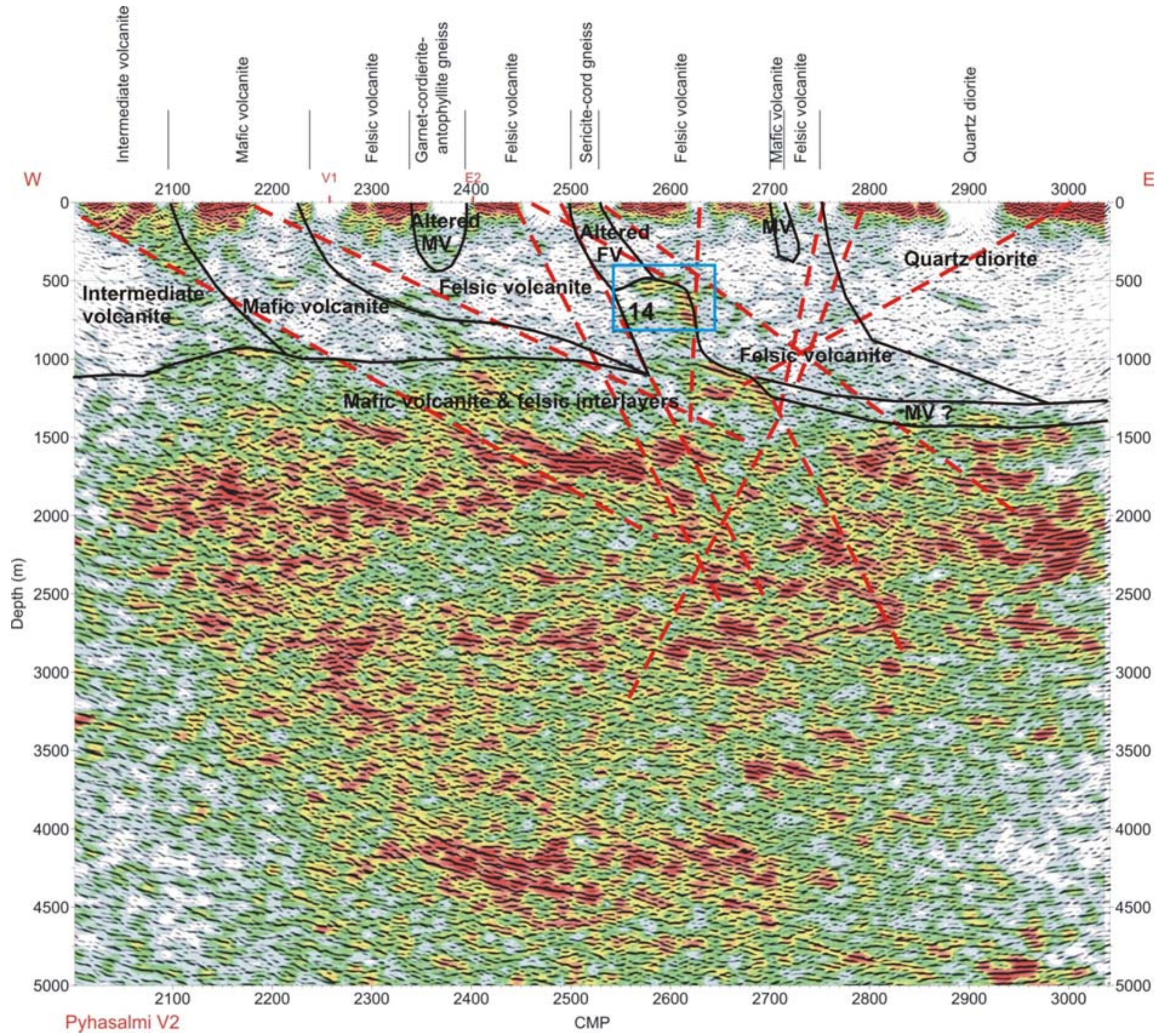

Figure 11. *Migrated NMO section of line V2 and its interpretation. Data representation and geological boundaries as in Fig. 8. FV: felsic volcanic rocks, MV: Mafic volcanic rocks.*

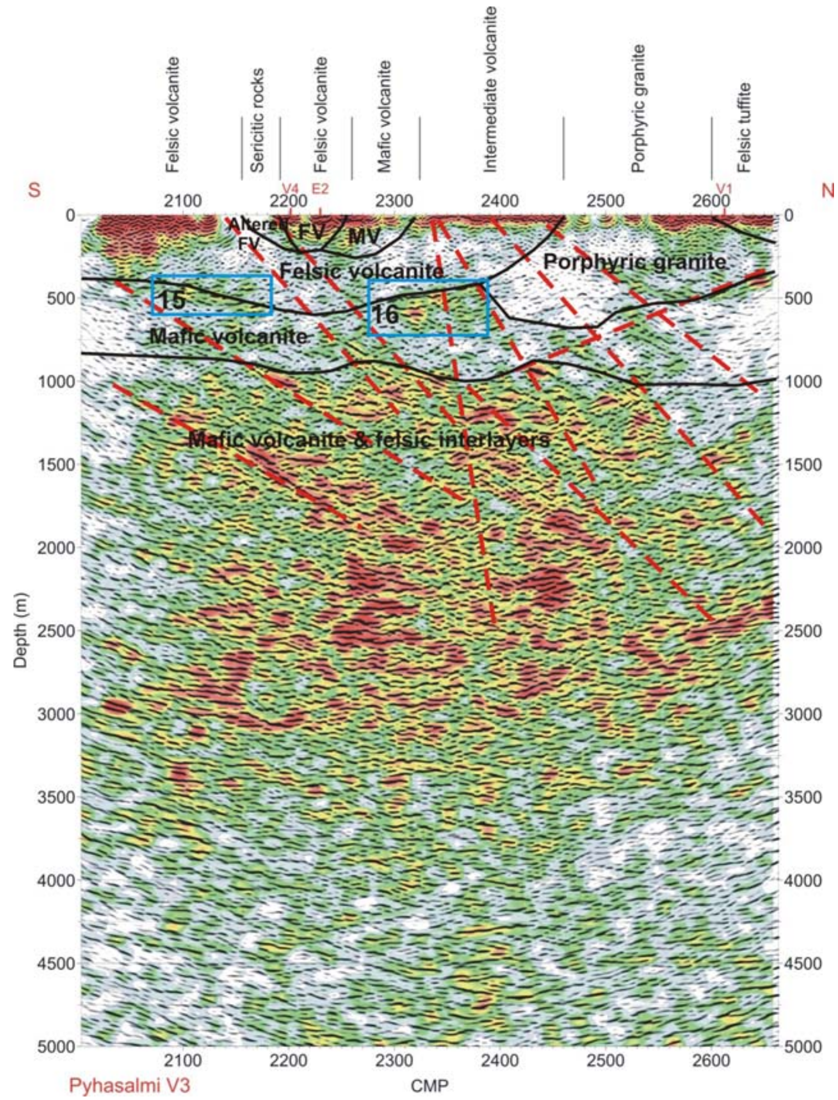

Figure 12. *Migrated NMO section of line V3 and its interpretation. Data representation and geological boundaries as in Fig. 8. FV: felsic volcanic rocks, MV: Mafic volcanic rocks.*

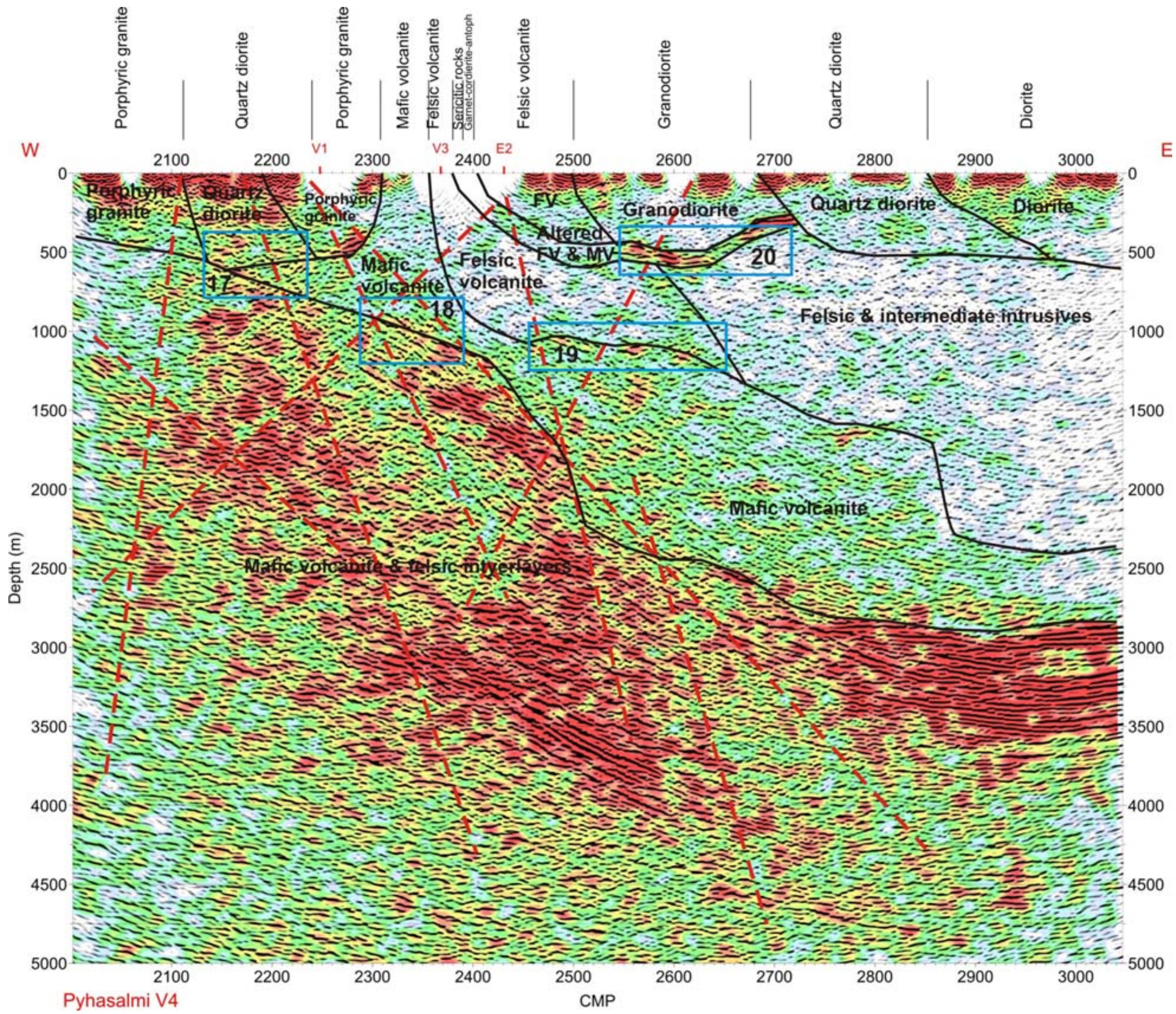

Figure 13. *Migrated NMO section of line V4 and its interpretation. Data representation and geological boundaries as in Fig. 8. FV: felsic volcanic rocks, MV: Mafic volcanic rocks.*

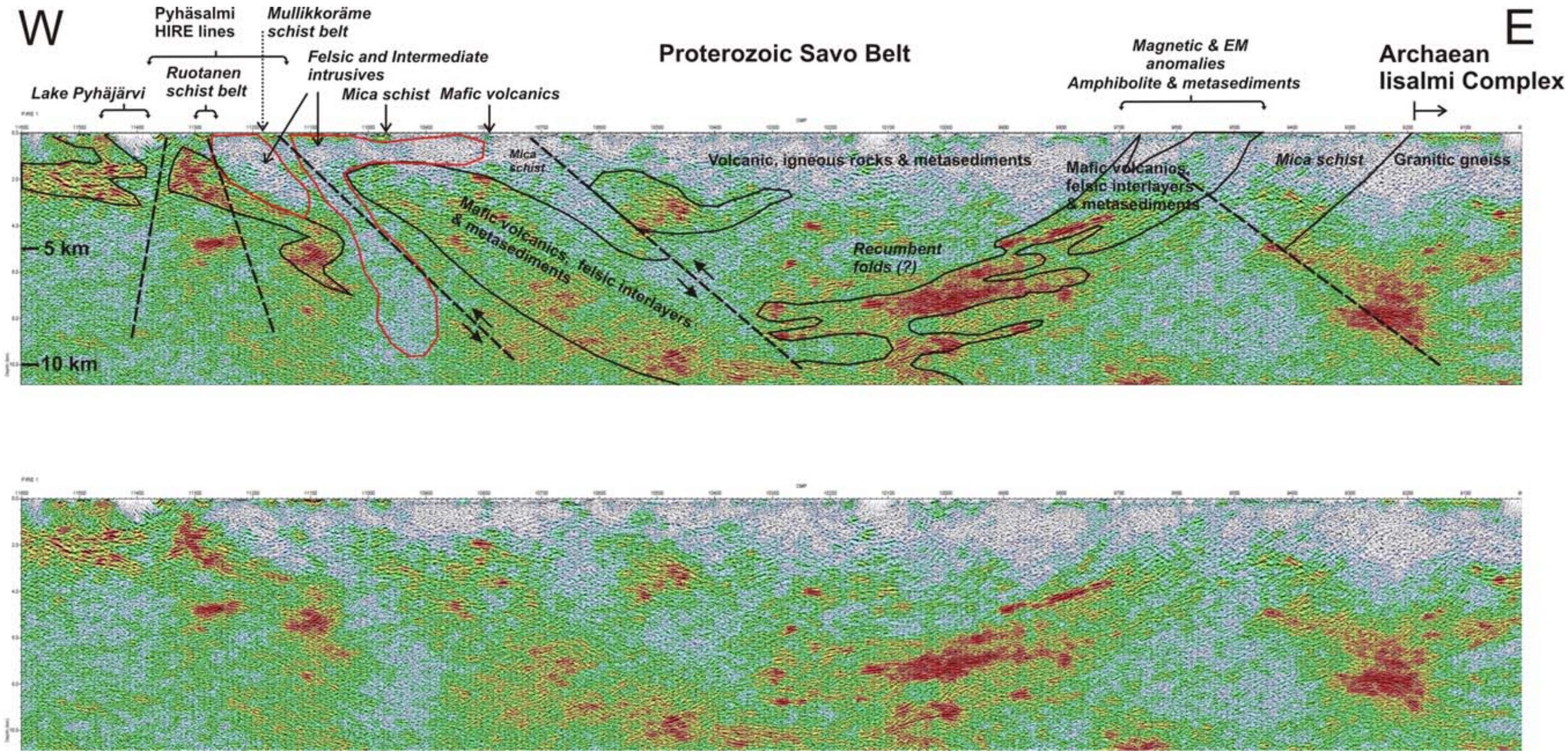

Figure 14. Part of FIRE-1 transect across the Savo Belt. A schematic interpretation of the reflectors is given. Black solid lines indicate strong reflective packages likely representing mafic volcanic rocks, felsic interlayers and metasediments, and red lines delineate felsic and intermediate igneous rocks, respectively. Broken lines show interpreted faults. The lower panel shows the section without interpretations for comparison. The vertical and horizontal scales are 1:1. The seismic data is from Kukkonen et al. (2006).

5.2. General reflection properties of the upper crust in the Pyhäsalmi area

Comparison of FIRE and HIRE data. The general result of the Pyhäsalmi HIRE data is the east dipping strong reflector system beneath a poorly reflective 1-2.5 km thick layer. The strong reflectors are wavy in details and show variations in reflection amplitude which gives an impression that they are not lithologically or structurally homogeneous (Figs. 8-13). They comprise reflective elements with vertical distances of about 40-60 m from each other, and horizontally the individual reflectors and reflective packages are 1-2 km long. The reflection texture is probably due to strong deformation, spatially varying dip angles and strikes (cross-dip effects) as well as compositional variations.

A regional framework for the HIRE results can be obtained from the FIRE-1 transect (Kukkonen et al., 2006), which runs across the Savo Belt in E-W direction (Fig. 14). The upper crustal reflectors of the Savo Belt form a synform about 50 km wide and 10 km deep. In earlier studies (Kukkonen at al., 2006; Korja et al., 2006) the synform reflectors were correlated with 1.88-1.93 Ga metavolcanic rocks of the Savo Belt. The strong reflectors detected in the present HIRE data in the Pyhäsalmi area are in the westernmost part of this large-scale synform structure.

The strong reflectors of the synform can be correlated with surface geology in the eastern part of the Savo Belt in the Kiuruvesi area where amphibolite (mafic metavolcanite) and mica schist occur (Fig. 14). Magnetic anomalies and good EM conductors suggesting the presence of black schist are also associated to these structures. In the western end of the synform, where the extrapolated reflectors should reach the surface, mafic volcanics and metasediments are shown on the 1:100 000 geological map (Marttila, 1992) in the vicinity of the E4 highway on the western side of Lake Pyhäjärvi. However, the correlation is complicated by the transect geometry, because the FIRE-1 profile takes a 80° turn at the northern end of Lake Pyhäjärvi.

The reflector synform of the Savo Belt suggests that considerable shortening has taken place in E-W direction, and several deep, mostly east-dipping (thrust) faults can be identified between Pyhäsalmi and the Archaean-Proterozoic boundary. Blocks of the strong reflector system seem to have been upthrusted by 1-2 km. In the central part of the synform at the depths of 5-10 km the reflectors may be interpreted as recumbent folds (Fig. 14). The Ruotanen Schist Belt and the Mullikkoräme Schist Belt are both located in the immediate vicinity of interpreted deep faults and boundaries of up-thrown blocks.

The strongly reflective zone detected on the FIRE-1 profile does not outcrop in the HIRE profiles. The regional correlation of the regional synform reflectors is supported by deep holes drilled from the mine which suggest that the strong HIRE reflectors would represent mafic volcanic rocks with felsic interlayers at least in the uppermost part of the reflective layer (see also discussion in chapter 5.4). This interpretation was applied in Figs. 8-13. The presence of metasediments too is suggested by the FIRE data above, but metasediments have not been reported from the drill holes in the mine.

Large poorly reflective (seismically transparent) areas located to the east of Pyhäsalmi in FIRE-1 correlate with felsic and intermediate intrusives on the surface. They extend to depths of several kilometres (Fig. 14), particularly in zones of thrusting. The same structures are seen in more detail on HIRE line V4 (Fig. 13).

Strongly vs. poorly reflective zones. The poorly reflective zone which extends from the surface to about 1-2 km level in the HIRE sections does not show good reflectors and is therefore difficult to correlate in detail with the surface geology. We attribute the lack of reflections to the generally steep attitude of the rocks which is not optimal for reflection surveys. The results very probably are due to a general difference between dip angles of strata of the poorly reflective areas (subvertical and steep dips) and the strongly reflective areas (subhorizontal to moderate dips).

Lithological differences are also present between the areas of poor and strong reflectivity as indicated by surface geology and deep drilling. Mainly the poorly reflective parts represent felsic and (massive) mafic volcanic rocks (both altered and unaltered) as well as felsic and intermediate intrusions, which seem to have small internal and mutual seismic impedance contrasts, i.e., they are seismically homogeneous rocks. On the other hand, the strongly reflective layer beneath 1-2 km is considered as mafic volcanic rocks with frequent felsic interlayers which therefore show much bigger internal impedance contrasts.

The different rock types, seismic data and the differences in structure and reflectivity could imply that the poorly and strongly reflective layers have behaved differently during upper crustal shortening and thrusting. The strong reflectors which are interpreted as dominantly mafic volcanic rocks would have been mainly competent whereas the felsic volcanic rocks and altered volcanics would have behaved incompetently during deformation. In a shortening system, this would result in brittle block movements of the competent units and (isoclinal) folding and shearing of incompetent rock units. Such a situation would be characteristic particularly for areas where the shortening has resulted in large antiform structures of the strongly reflective layer, for instance beneath the Ruotanen Schist Belt (Fig. 8). It should be noted that the structures hosting the sulphide deposits in the uppermost 1.5 km of the Ruotanen Schist Belt have been geologically interpreted as a synform-antiform structure (Mäki et al., 2002; Fig. 2). This interpretation was followed in the present modelling (Fig. 8).

5.3. Reflection imaging of the Pyhäsalmi ore deposit

The Pyhäsalmi deposit is a subvertical structure extending from the surface as a thin plate to about 1 km where it seems to thin out almost completely (Figs. 1 and 2). At depths exceeding 1.1 km the deposit thickens and widens again (the new deep ore). The deep ore is an elongated pear-shaped body which is 200 m wide, 400 m long and 320 m high, and the length of long axis is about c. 600 m. It is located very close to the crossing of lines V1 and E1 and touched by both lines (Figs. 8, 10 and 15).

The upper subvertical part of the deposit to a depth of 1 km has been mostly mined away. Some seismic response could in principle be expected from reflectivity generated by the host rock and mine gallery fillings, but the vertical structures are not favourable for the method. However, the conditions for the deep ore are different. Comparing Surpac images constructed from the seismic sections and the geological model of the ore body (obtained from Pyhäsalmi Mine Oy) shows that the deep ore is located at the upper margin of a strong reflector package (Figs. 8 and 10). The ore body appears to be partly surrounded by strong reflectors from below as well as from its eastern and northern sides. Also there seems to be a reflector from the lower contact of the upper end of the deep ore (i.e., the narrow end of the 'pear'). The nearby strong reflectors beneath and to the E of the deep ore body seem to form an antiform-like structure.

Was the deep ore body directly imaged? A massive sulphide ore body has a strong reflectivity contrast with any normal rock type, and should be detectable if the body is only big enough. Wave theory requires that a reflector located at 1.0 km depth must be vertically thicker than 10 m and horizontally wider than 270 m to be detectable with seismic waves. Here we have assumed an average velocity of 6000 m/s and wave frequency of 165 Hz. The vertical dimension of the deep ore body is sufficient for detection but the problem is the horizontal dimension which is about the same order of

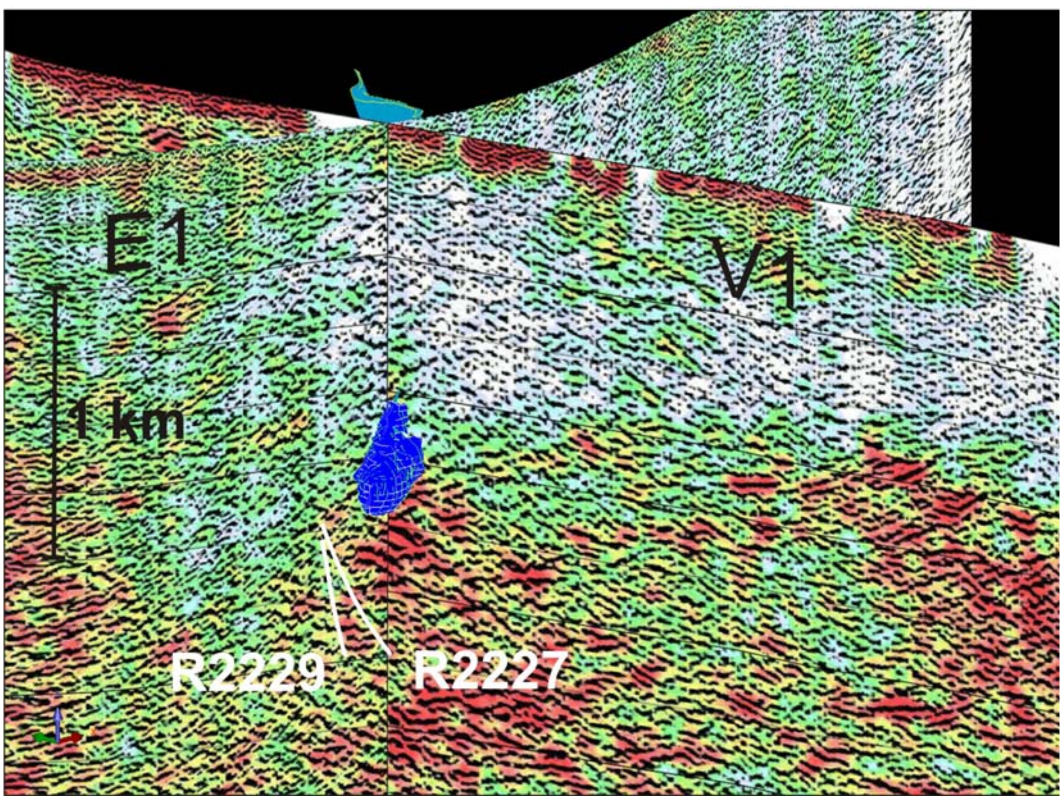

Figure 15. *Surpac view from SW of the lines E1 and V1. The ore deposit is shown with blue colour. Two deep holes intersecting upper parts of the strong reflector system are included (cf. Fig. 16).*

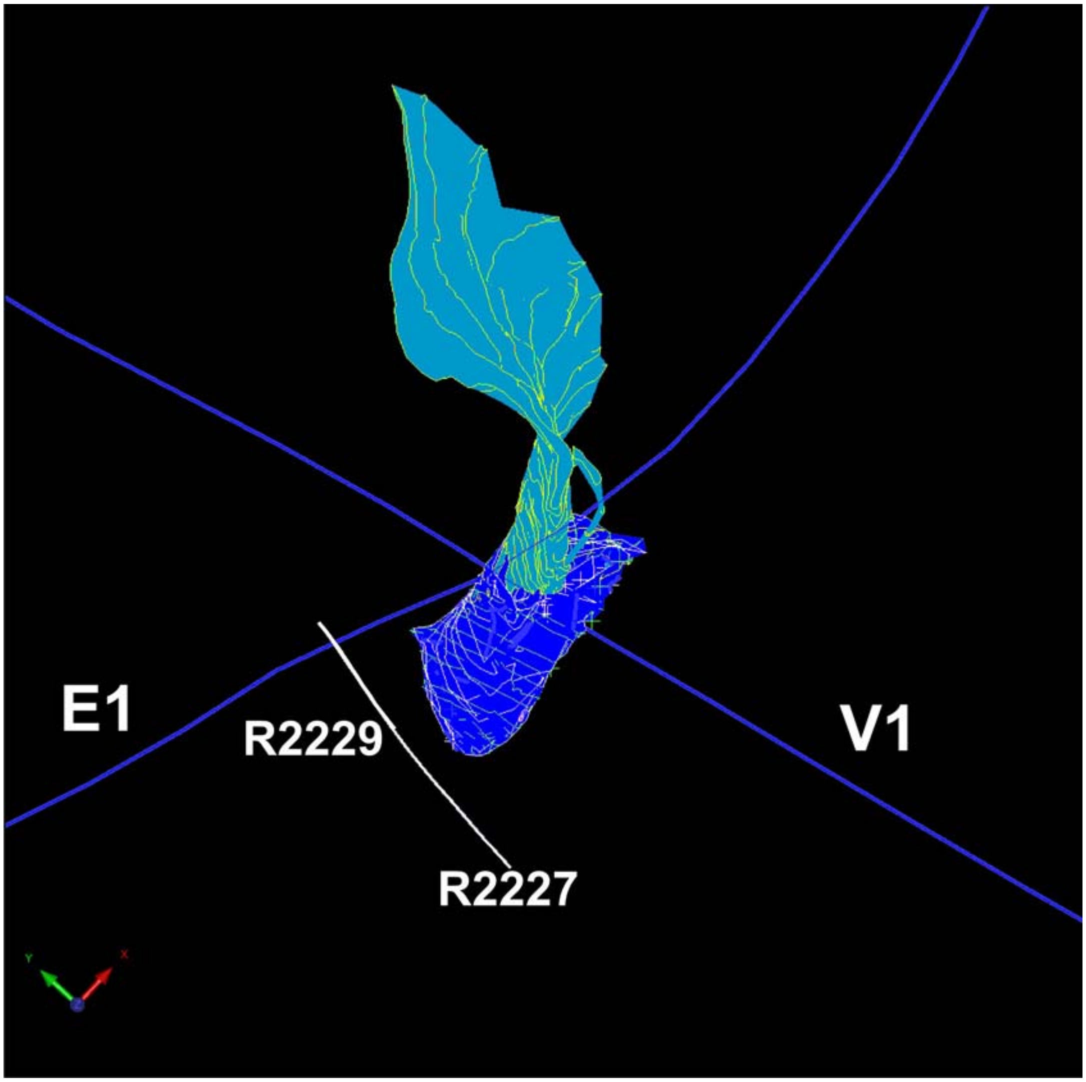

Figure 16. *Projection of lines E1, V1, the Pyhäsalmi ore deposit and drill holes R2229 and R2227 on a horizontal x-y plane (cf. Fig. 15).*

magnitude as the required theoretical minimum dimension. The response of the deep ore body is also influenced by the shape of the body. The upper surface is not flat, but formed by the N and S sides meeting at an angle, whereas the lower surface is much more flatter. This may be the reason for strong reflections from the basal contact zone but very weak reflections from the upper surface. On the other hand, there are reflections from the sides which also agree with the overall shape of the ore body. We may conclude that the deep ore body was directly imaged with reflection, but nevertheless its response is not obvious on the NMO sections (Figs. 8 and 10). The observed reflectivity is geologically due to impedance contrast between, on one hand, the massive sulphides and its host rocks (mafic volcanic rocks and interlayers of felsic rocks), and on the other hand, to internal reflection contrasts within the host rocks. The subhorizontal position of these lithologies further enhances the reflectivity beneath the deep ore.

5.4. Comparison of drill hole data and reflectors

Drill hole data from boreholes R2227 and R2229 (Figs. 14 and 16) indicate that the rocks beneath the deep ore are dominantly mafic volcanic rocks with interlayers of felsic volcanics, pegmatite, tonalite and skarn. The thicknesses of interlayers range from a few metres to about 25 m. Also thin (<5 m) shear zones are met with. Although we have no *in situ* velocity and density data from the drill holes, we can assume that there is a seismic impedance contrast between the mafic volcanic rocks and the more felsic and intermediate rocks. This is supported by comparison of the lithological column of R2229 and the corresponding seismic trace from the NMO migrated section E1 (Fig. 16).

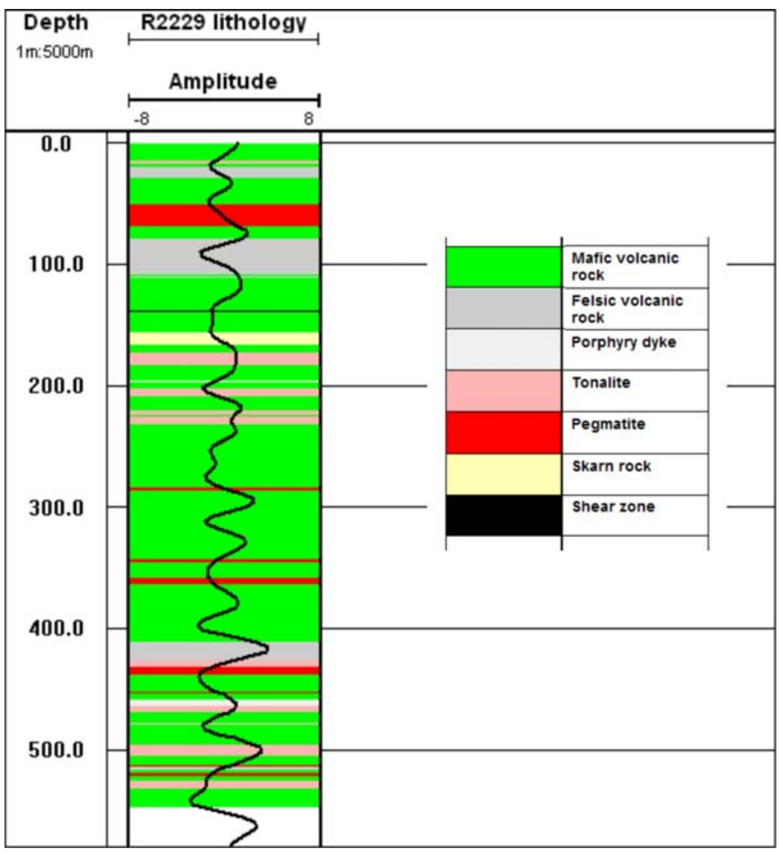

Figure 17. *Comparison of lithologies of drill hole R2229 and the corresponding seismic trace at CMP 2395 on line E1 (migrated NMO section). The depth scale of the trace was matched with depths of the drill hole inclined about 70º. The drill hole collar elevation is -1280 m (national kkj grid system). Compare with Fig. 15.*

Two other drill holes (R2226 and R2228), which have moderate dip angles, are shown in Figs. 18 and 19 and their lithologies in Fig. 20. These holes are much more difficult to compare with the seismic sections, but some notes can be given. Both holes are expected to be within the strongly reflective layers detected on E1 and E2. The lithological variation in both holes shows layers ranging in thickness from a few meters to tens of metres, and the lithologies represent mainly felsic volcanic rocks with interlayers of pegmatite, mafic volcanic rocks, tonalite, skarn and thin shear zones. The expected variation in acoustic properties could well generate the strong reflectivity.

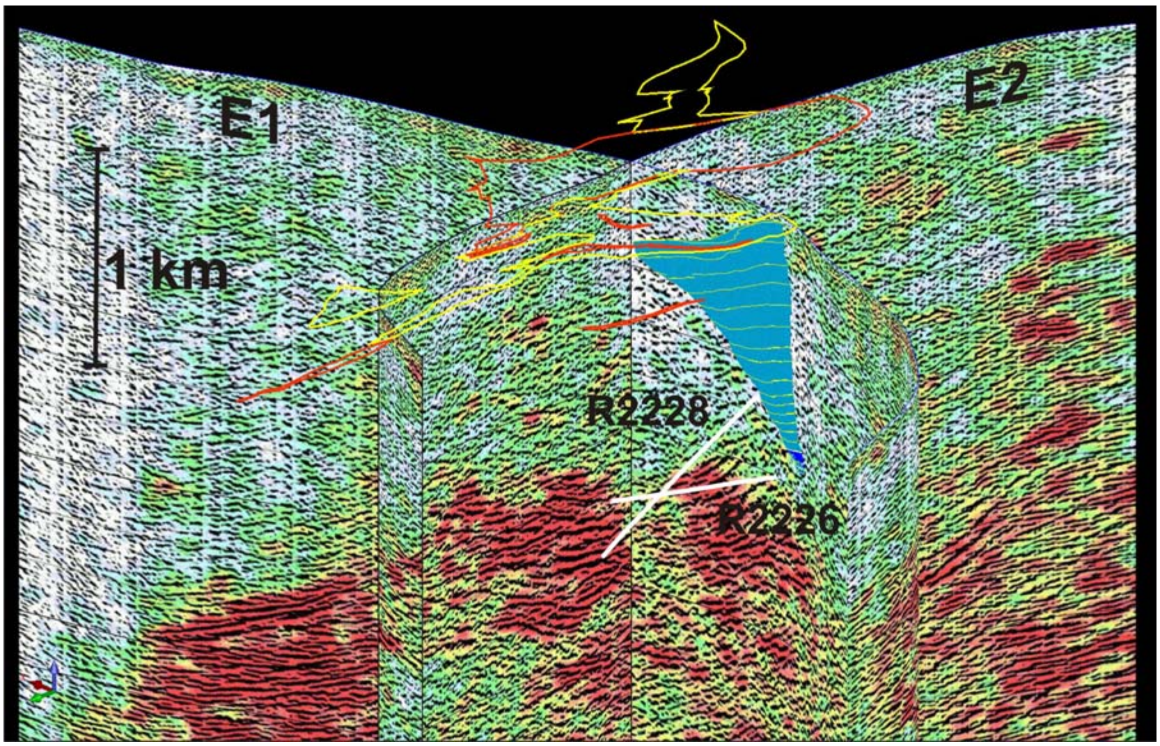

Figure 18. *Perspective view of lines E1 and E2 from NW with the drill holes R2226) and R2228. The red and yellow lines indicate the distribution of cordierite-antophyllite rock and sericite schist on the surface level.*

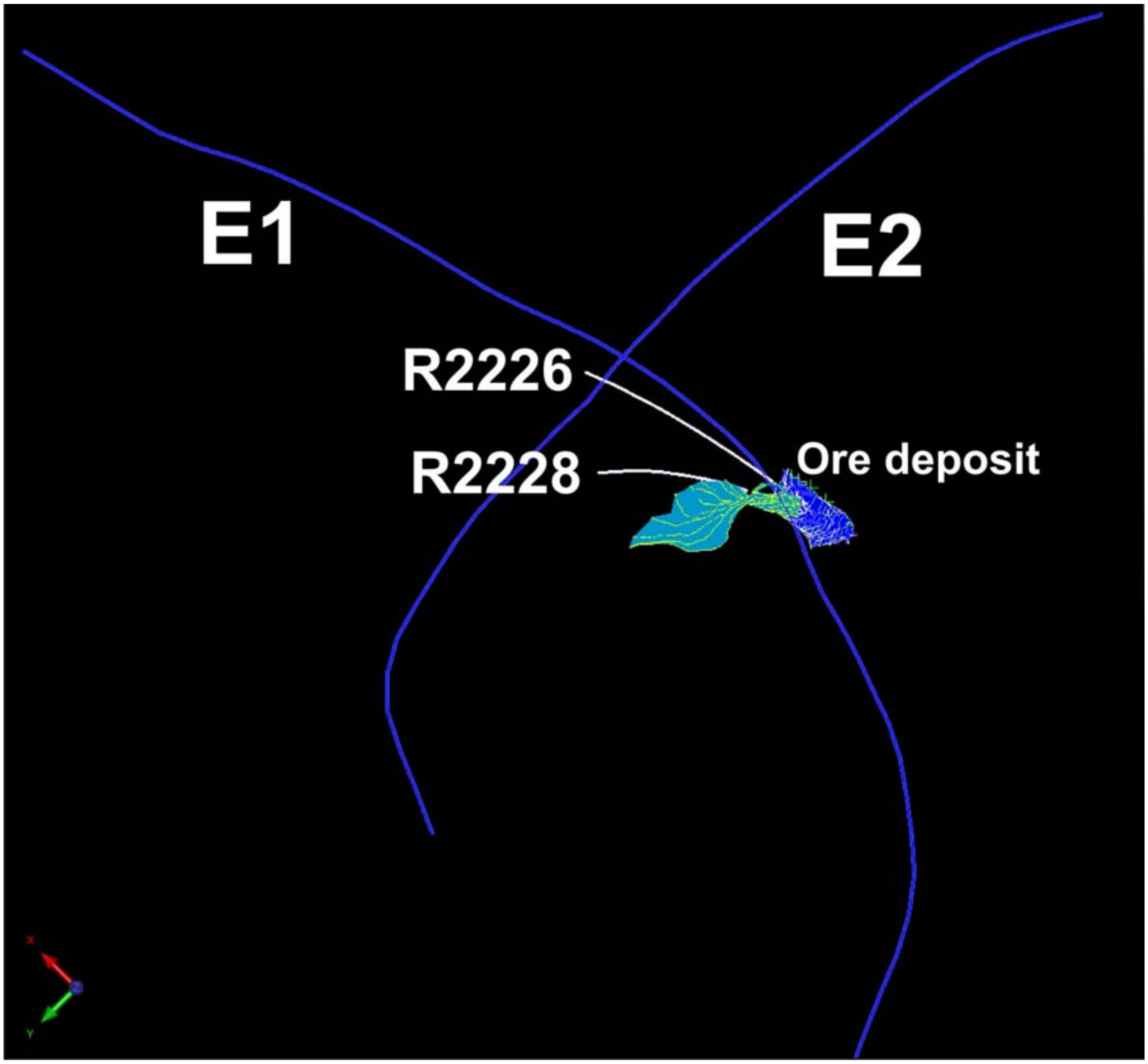

Figure 19. *Projection of lines E1 and E2, the Pyhäsalmi ore deposit and drill holes R2226 and R2228 on a horizontal x-y plane (cf. Fig. 18).*

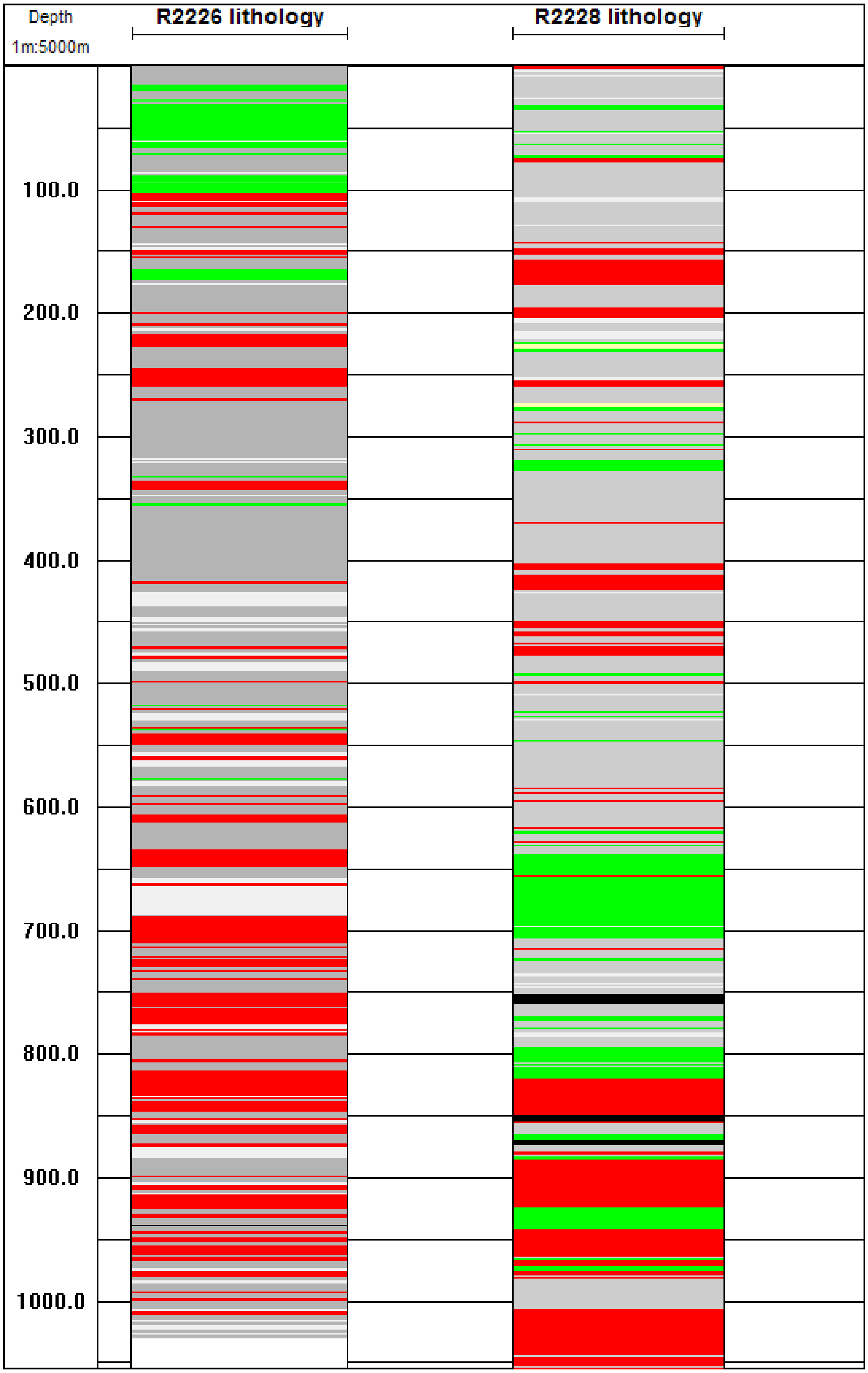

Figure 20. *Lithological columns of drill holes R2226 (collar elevation -1067 m, national kkj grid) and R2228 (collar elevation -688 m). The legend of the colors is the same as in Fig. 15.*

6. Discussion

6.1. Reflective structures, altered rocks and the Pyhäsalmi ore deposit

In the upper parts of the Pyhäsalmi mine the mineralizations and deposits are hosted by hydrothermally altered rocks, i.e., mainly sericite schist and cordierite-antophyllite rock, which were altered from felsic and mafic volcanic rocks, respectively. The deep ore body, on the other hand, is hosted by mafic and felsic volcanic rocks and pegmatite. This may be attributed to intensive deformation and strain in the deeper parts of the deposit, as well as to mobilization of the ore during metamorphic deformation.

The genesis of the Pyhäsalmi ore was related to hydrothermal alteration in volcanic strata. Felsic rhyolitic volcanism was followed by mafic tholeiitic volcanism and sulphide mineralization took place early in a rifted marine environment by extensive hydrothermal circulation near mafic volcanic centres. The originally thin ore layer was thickened and deformed tectonically into its present form (Kousa et al., 1997; Luukas et al., 1999; Mäki et al., 2002; Rasilainen et al., 2003). According to this view the original mineralization had a stratigraphic control and it was located in the boundary zone between felsic and mafic volcanics.

Although the stratigraphy in Pyhäsalmi is unclear (Kousa et al., 1997; Luukas 1999), the mafic volcanics mapped on the surface, in drill holes and underground seem to be younger than the felsic volcanics. We have no exact information how the deep strongly reflective layers interpreted here to represent mafic volcanics and felsic interlayers relate to the (mostly) more massive mafic volcanics mapped on the surface and in the mine. They may basically represent different levels of a volcanostratigraphic system but could also represent the same stratigraphic level with only different degrees of deformation. In this view the stratigraphic top is most probably directed generally downward. Whether this is the rule in the regional synform characterizing the Savo Belt, remains an open question, but it is a feasible hypothesis as the early isoclinal recumbent folding is known to have thickened the ore (Mäki et al., 2002) and overturned the strata. The FIRE-1 regional seismic data also suggest that recumbent folds are possible in the deep parts of the Savo Belt synform (Fig. 14). In such a model the mineralizations should be found at the boundary zone between the felsic and mafic volcanic rocks where altered volcanic rocks are expected to occur. Locating such contacts in the seismic sections is, however, not straightforward because the lithological interpretation of the reflectors is not unique. Nevertheless, we can consider that the contact zone should follow the upper boundary of the strongly reflective layer or to be above the boundary. The Pyhäsalmi deep ore body is located in this zone, although it has been strongly affected by post-depositional deformation and possibly by mobilization of sulphides.

A number of up-thrusted blocks (‘protrusions) of reflectors which extend from the upper surface of the strongly reflective zone correlate with the surface distribution of the altered rocks on lines E1, V2 and V4 (Figs. 8, 10, 13 & 19). It is possible that the boundaries of these blocks represent shears connected to the zones altered rocks at the surface level.

The protrusions follow a SE-NW strike and coincide with the grain of the magnetic anomalies on the western side of Lake Komujärvi. The up-thrusting of the blocks is in line with the interpretation of the FIRE-1 data (chapter 5.2 and Fig. 14).

The Pyhäsalmi ore deposit is located in the upper boundary of the strongly reflective zone. On the E-W oriented section E1 the deposit is sitting on the western flank of an antiform-like structure of reflectors (Fig. 8). The deposit size is on the limit of detectability with seismic reflections, but the detailed analysis of the migrated (and unmigrated) stacks of lines E1 and V1 (Figs. 8 and 10) suggests that the deposit was directly imaged.

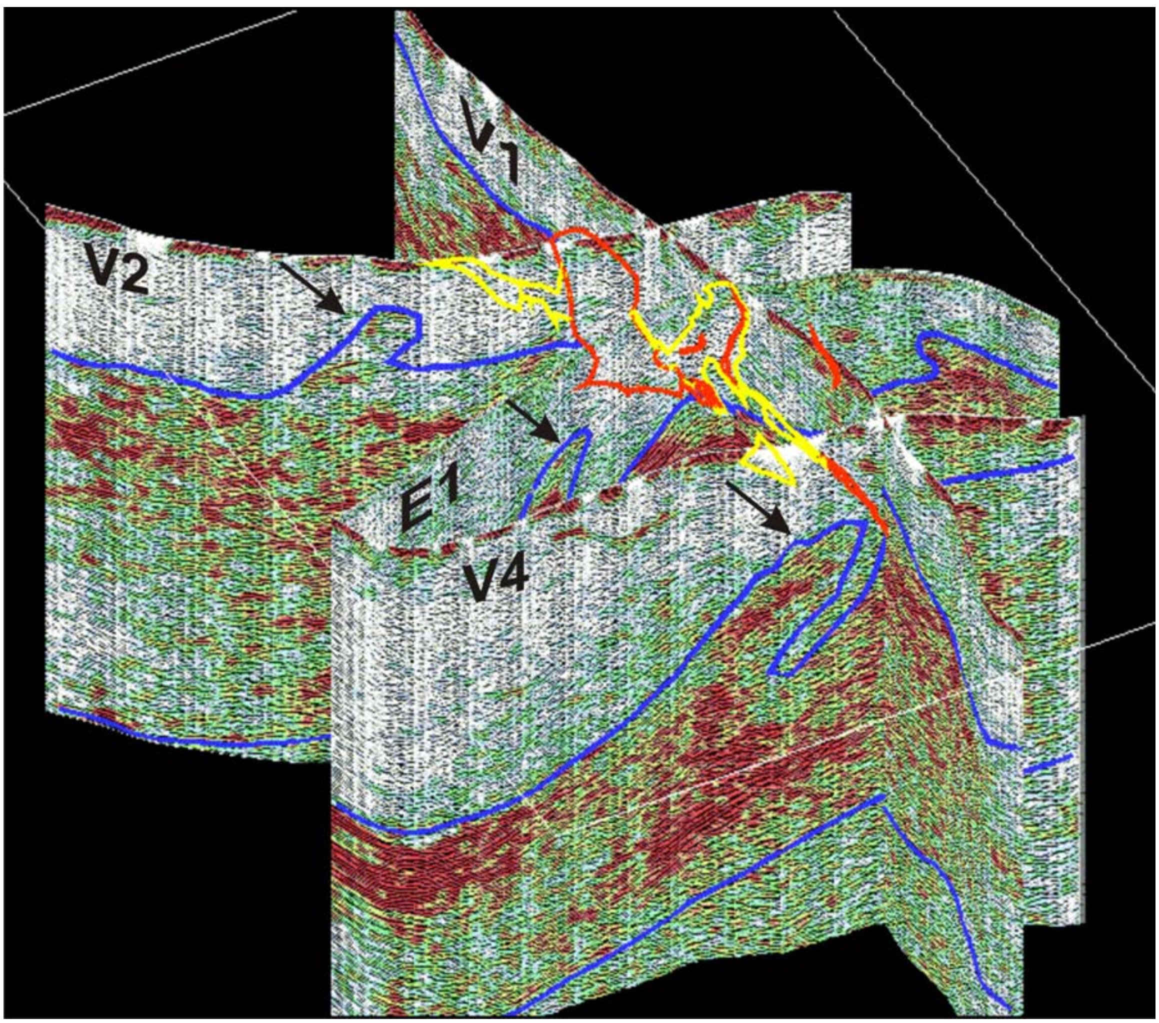

Figure 21. *Perspective view of lines V1, V2, V4 and E1 from NE together with surface loops of altered rocks (red: cordierite-antophyllite rock, yellow: sericite-schist). The upward protrusions of the strongly reflective layer indicated with arrows correlate with surface zones of altered rocks.*

The possibility of mineralizations on the eastern flank of the antiform structure hosting the deep ore on E1 should also be considered. However, the hole R2226 which approximately follows the E1 section (Figs. 17 and 18) does not show any major deposits related to these reflectors, although altered rocks were encountered. Instead, the drilling data suggested that the existing lithologies may generate the observed reflectivity (see discussion in chapter 5.4). There is a possibility that the reflector on the eastern side of the deep ore body (Fig. 8) would be generated by a cross-dip effect due to a reflector located away from the vertical plane. The drill hole R2228 intersected the expected space of the reflectors on the NW side of the E1/E2 crossing, but it shows only alternating layers of felsic and mafic volcanics and pegmatite in the lower part of the hole (Fig. 19).

The geological nature of the strongly reflective layer beneath 1-2 km level in the Pyhäsalmi area is not clear, but it most likely represents mafic volcanic rocks interlayered by felsic volcanics, and cut by pegmatite. This was supported by the geological data from the drill holes R2227 and R2229 (Figs 16 and 17). Such lithologies are expected to easily generate the observed reflectivity. As the up-thrusted blocks spatially correlate with mineralized altered rocks on the surface (Figs. 8, 10, 13), it is tempting to interpret that such rocks would also be common in the vicinity of the upper boundary of the strong reflector system. This is, however, only speculation, but encourages attempts to find out the geological character of the deep reflectors.

The strong reflector system does not outcrop in the study area. Extrapolating the reflector in V4 along its dip angle to the surface suggests that the reflectors should outcrop under the Lake Pyhäjärvi, whereas V2 indicates a more or less horizontal position. The crustal scale FIRE-1 data shows apparently subhorizontal reflectors continuing to the W and SW from Pyhäsalmi at the depth of about 1.5 km, but there is a possible surface contact on the western shore of Lake Pyhäjärvi (Fig. 14). Further, extrapolated surface contacts of the strong reflector may be present in the vicinity of the E4 highway where mafic volcanic rocks and metasediments occur on the 1:100 000 geological map (Marttila, 1992). Therefore metasedimentary rocks may also be a component of the strongly reflective layer in the HIRE data.

6.2. Suggestions for further exploration

The present data set indicates several potential structures for further exploration. We have selected some of them in Table 7 and indicated them in Figs. 8-13. Here it must be taken into account that the geological data was very limited in the modelling of the rock type boundaries shown, and the presented interpretations in Figs. 8-13 should be taken with caution.

Table 7. Suggested targets for further exploration.

Target[1]	Line	CMP	Depth (m) below datum[2]	Description
1	E1	2150	600-800	Possible analoguous site for the deep ore body
2	E1	2280	600-800	Reflector at mafic/intermed.volcanite contact
3	E1	2590	1250-1400	Possible analoguous site for the deep ore body
4	E1	2730	800-1250	Top of upthrusted block, area of altered rocks
5	E2	2070	400-600	Reflector at mafic/felsic volcanite contact
6	E2	2180	500-800	Reflector at mafic/felsic volcanite contact
7	E2	2410	600-1000	Reflector at contact of mafic volc./altered mafic volc. contact
8	E2	2550	400-750	Reflector at contact of mafic volc./altered mafic volc. contact
9	E2	2820	800-1250	Reflector mafic/felsic volcanite contact
10	V1	2250	600-1000	Possible analoguous site for the deep ore body
11	V1	2420	250-500	Reflector at mafic/felsic volcanite contact
12	V1	2540	250-500	Reflector at mafic/felsic volcanite contact
13	V1	2900	400-800	Upper boundary of strong reflector system
14	V2	2580	400-800	Reflector at top of upthrusted block, area of altered rocks
15	V3	2130	400-600	Reflector at mafic/felsic volcanite contact
16	V3	2330	400-700	Reflector at mafic/felsic volcanite contact
17	V4	2180	400-750	Reflector at top of upthrusted block, under quartz diorite
18	V4	2330	750-1200	Reflector at top of upthrusted block, possibly an area of altered rocks
19	V4	2550	900-1250	Reflector at mafic/felsic volcanite contact
20	V4	2620	300-700	Reflector below granodiorite, possibly altererd rocks

[1] The targets are marked in Figs. 8-13 and also included in the *Surpac* materials for easy application.
[2] The datum level is +150 m a.s.l.

Generally, the suggested exploration targets can be divided in three main groups:

(1) Possible analogous sites of the deep ore body along the upper boundary of the strongly reflective layer (targets 1, 3, 10, 13 and 17);
(2) Reflectors at interpreted mafic/felsic volcanic rock contacts located mostly within the weakly reflective layer (targets 2, 5-9, 11, 12, 15, 16, and 19);
(3) The structures of the up-thrusted blocks which are associated with altered volcanic rocks on the surface (targets 4, 14, and 18); and
(4) Other types: Flat reflectors under intrusive rocks (target 20)

7. Conclusions

The HIRE seismic reflection survey provided a detailed image of seismic reflectivity of the Pyhäsalmi mining area and its surroundings. Distinct new data on the deep structure were obtained. Numerous previously unknown structures were discovered.

The most prominent feature in the HIRE results is the bimodal general characteristics of the reflectivity. An E-NE dipping strongly reflective layer was detected at depths exceeding 1-2.5 km. Above this layer the reflectivity is very weak and not simple to correlate with surface geology. The strongly reflective layer consists of reflective elements which are at about 40-60 m vertical distances from each other. Drill hole data (R2227 and R2229) suggest that the reflectivity could be attributed to mafic volcanic rocks with interlayers of felsic volcanics and pegmatite dykes.

Using large-scale reflection seismic data of the FIRE-1 transect the strongly reflective system can be correlated with a 50 km wide and 10 km deep synform structure of the Savo Belt. Surface geology suggests that the synform and the strongly reflective layer represent mafic volcanic rocks with felsic interlayers as well as metasediments. Considerable shortening has taken place in E-W direction, and several deep, mostly east-dipping (thrust) faults can be identified between Pyhäsalmi and the Archaean-Proterozoic boundary. The Ruotanen and the Mullikkoräme Schist Belts are both located in the immediate vicinity of interpreted deep faults and boundaries of up-thrown blocks.

The Pyhäsalmi deep ore deposit is located at the upper boundary of the strongly reflective zone where the reflectors beneath the deposit seem to form an antiform-like structure. The reflection image of the pear-shaped deep ore body at the depth of 1.1 - 1.5 km is characterized by strong reflectors beneath and on the eastern side of the massive ore. The observed reflectivity is geologically due to impedance contrast between, on one hand, the massive sulphides and its host rocks (mafic volcanic rocks and interlayers of felsic rocks), and on the other hand, to internal reflection contrasts within the host rocks.

Assuming that there originally has been a stratigraphic control of the sulphide deposits at the contact zone between older felsic volcanic rocks and younger mafic volcanics, the reflection data can be used to indicate possible targets for exploration. These can be divided in three main groups. *First*, the location of the Pyhäsalmi deep ore deposit at the upper boundary of the strongly reflective layer encourages seeking for analogous sites along the reflector boundary. *Second*, the presented correlation of lithological boundaries at surface level with the HIRE seismic results suggested several potential exploration targets at interpreted mafic/felsic volcanic rock contacts. *Third*, the structures of the up-thrusted blocks which are associated with altered volcanic rocks on the surface are also potential targets for exploration.

References

Ekberg, M. & Penttilä, V-J. 1986. The Pyhäsalmi Cu-Zn-pyrite deposit. In: Gaál, G. (ed.) Proterozoic Mineral Deposits in Central Finland. 7th IAGOD Symposium and Nordkalott Project Meeting (Luleå, 1986): Excursion Guide no 5. Sveriges Geologiska Undersökning. Ser. Ca 63, 20-25.

Helovuori, O. 1979. Geology of the Pyhäsalmi ore deposit, Finland. Economic Geology 74, 1084-1101.

Inmet Mining, 2008. Annual Report, 2008. Reserve data given in the web at:
http://www.inmetmining.com/Theme/Inmet/files/pdf/2008_Mineral%20Reserves%20and%20Resources.pdf

Korja, A., Lahtinen, R., Heikkinen, P., Kukkonen, I.T. and FIRE Working Group, 2006. A geological interpretation of the upper crust along FIRE 1. In: Kukkonen, I.T. and Lahtinen, R. (editors), Finnish Reflection Experiment 2001-2005. Geological Survey of Finland, Special Paper 43, pp. 45-76 and 1 appendix.

Kousa, J., Luukas, J., Mäki, T., Ekdahl, E., Pelkonen, K., Papunen, H., Isomäki, O-P., Penttilä, V-J. & Nurmi, P. 1997. Geology and mineral deposits of the central Ostrobothnia. Geol. Surv. Finland, Guide 41, 43-67.

Kukkonen, I.T., Heikkinen, P., Ekdahl, E., Hjelt, S.-E., Yliniemi, J., Jalkanen, E. and FIRE Working Group, 2006. Acquisition and geophysical characteristics of reflection seismic data on FIRE transects, Fennoscandian Shield. In: Kukkonen, I.T. and Lahtinen, R. (editors), Finnish Reflection Experiment 2001-2005. Geological Survey of Finland, Special Paper 43, pp. 13-43 and 11 appendices.

Luukas, J., Puustjärvi, H. & Kousa, J., 1999. Pyhäsalmi Modeling Project, Geology. In: H. Puustjärvi (ed.), Pyhäsalmi Modeling Project 13.5.1997-12.5.1999, Outokumpu Mining Oy & Geological Survey of Finland, Unpublished project report, section B, pp. 1-66.

Marttila, E., 1992. Pre-Quaternary rocks 1:100 000, Map Sheet 3321, Pyhäjärvi. Geological Survey of Finland, Espoo.

Mäki, T. & Luukas, J. 2001. Structural control of the Pyhäsalmi VMS deposit in the Palaeoproterozoic Raahe-Ladoga Zone, central Finland. In: Williams P.J. (ed.) 2001: A Hydrothermal Odyssey. May 17-19th, 2001, Townsville. Extended abstracts. EGRU and JCU. 122-123.

Mäki, T., Lappalainen, M., Brusila, J., Mäkinen, I. & Lähteenmäki, S., 2002. 2001 Report on Estimated Mineral Reserves and Resources, Pyhäsalmi Mine. Inmet Minining Corporation, Toronto, Technical Report (supervised by F. Balint & J. Boaro), May 17, 2002, 41 p.

Rasilainen, K., Puustjärvi, H., Kousa, J., Luukas, J. & Mäki, T., 2003. The Paleoproterozoic Pyhäsalmi volcanic complex, central Finland – Bimodal volcanism and associated VMS deposits. In: D.G. Eliopoulos et al. (eds.), Mineral Exploration and Sustainable Development, Vol.2, Proceedings of the Seventh Biennal SGA Meeting, Athens, Greece, 24-28 August, 2003, pp. 1095-1098.

Zamoshnyaya, N. and Sorokina, G, 2008. Report on the HRSS 2D reflection survey carried out in Finland during 2008 – Vihanti, Pyhäsalmi and Kevitsa (Volume 1). Federal State Unitary Geological Research-and-Production Enterprise for Geophysical Works of the Russian ministry of Natural Resources, GFUP Vniigeofizika, AE Spetsgeofizika. Contract No. 50-0701/042362, Povarovka, Russia, 103 p.

Figures

Figure captions

Figure 1. Views of the Pyhäsalmi deposit (Image: T. Mäki, Pyhäsalmi Mine Oy).

Figure 2. Structure of the Pyhäsalmi ore deposit and the host rocks (Mäki et al., 2002)

Figure 3. The average velocity (red line) and measured stacking velocities (colored dots). The color of the dot indicates the line (E2, V1-V4). The vertical axis is the velocity in m/s and the horizontal axis is the two-way traveltime in milliseconds.

Figure 4. Survey lines in Pyhäsalmi. Numbers along the lines indicate receiver station pole numbers (italics) and CMP coordinates (normal text).

Figure 5. Relations between true and apparent dip angles of planar reflectors. The curve parameter is the angle between the survey line and the strike of the reflector at surface.

Figure 6. Frequency spectra of the vibrator field data from V1 with two offsets from the shot point. Upper panels: offset 150-200 m, lower panels: offset 1950-2050 m. (Zamoshnyaya, 2008). The shot point is at CMP 2698 above the deep ore.

Figure 7. Frequency spectra of the explosion seismic field data from E1 with two offsets from the shot point. Upper panels: offset 150-200 m, lower panels: offset 1950-2050 m. Shot point location (CMP 2642) is about 1 km to the east of the deep ore (Zamoshnyaya, 2008).

Figure 8. Migrated NMO section of line E1 and its interpretation. Reflectors with high amplitude are automatically enhanced with red background colour. Geological boundaries at the surface are from the geolocical database of GTK (1:200 000 scale bedrock geology). The boundaries of interpreted geological boundaries are shown with black lines. The red lines indicate interpreted shear and fault zones. FV: felsic volcanic rocks; AF: altered felsic volcanic rocks; MV: mafic volcanic rocks. The blue boxes with numbers indicate suggested exploration targets (Table 7).

Figure 9. Migrated NMO section of line E2. Data representation and geological boundaries as in Fig 8.

Figure 10. Migrated NMO section of line V1. Data representation and geological boundaries as in Fig. 8. FV: Felsic volcanic rocks.

Figure 11. Migrated NMO section of line V2. Data representation and geological boundaries as in Fig. 8. FV: Felsic volcanic rocks, MV: Mafic volcanic rocks.

Figure 12. Migrated NMO section of line V3. Data representation and geological boundaries as in Fig. 8. FV: Felsic volcanic rocks, MV: Mafic volcanic rocks.

Figure 13. Migrated NMO section of line V4. Data representation and geological boundaries as in Fig. 8. FV: Felsic volcanic rocks, MV: Mafic volcanic rocks.

Figure 14. Part of FIRE-1 transect across the Savo Belt. A schematic interpretation of the reflectors is given. Black solid lines indicate strong reflective packages likely representing mafic volcanic rocks, felsic interlayers and metasediments, and red lines delineate felsic and intermediate igneous rocks, respectively. Broken lines show interpreted faults. The lower panel shows the section without interpretations for comparison. The vertical and horizontal scales are 1:1. The seismic data is from Kukkonen et al. (2006).

Figure 15. Surpac view from SW of the lines E1 and V1. The ore deposit is shown with blue colour. Two deep holes intersecting upper parts of the strong reflector system are included (cf. Fig. 16).

Figure 16. Projection of lines E1, V1, the Pyhäsalmi ore deposit and drill holes R2229 and R2227 on a horizontal x-y plane (cf. Fig. 15).

Figure 17. Comparison of lithologies of drill hole R2229 and the corresponding seismic trace at CMP 2395 on line E1 (migrated NMO section). The depth scale of the trace was matched with depths of the drill hole inclined about 70º. The drill hole collar elevation is -1280 m (national kkj grid system). Compare with Fig. 15.

Figure 18. Perspective view of lines E1 and E2 from NW with the drill holes R2226) and R2228. The red and yellow lines indicate the distribution of cordierite-antophyllite rock and sericite schist on the surface level.

Figure 19. Projection of lines E1 and E2, the Pyhäsalmi ore deposit and drill holes R2226 and R2228 on a horizontal x-y plane (cf. Fig. 18).

Figure 20. Lithological columns of drill holes R2226 (collar elevation -1067 m, national kkj grid) and R2228 (collar elevation -688 m). The legend of the colours is the same as in Fig. 15.

Figure 21. Perspective view of lines V1, V2, V4 and E1 from NE together with surface loops of altered rocks (red: cordierite-antophyllite rock, yellow: sericite-schist). The upward protrusions of the strongly reflective layer indicated with arrows correlate with surface zones of altered rocks.

Appendices

1. Seismic survey lines plotted on the geological map
2. Seismic survey lines plotted on the airborne magnetic map
3. NMO migrated section of line E1
4. NMO migrated section of line E2
5. NMO migrated section of line V1
6. NMO migrated section of line V2
7. NMO migrated section of line V3
8. NMO migrated section of line V4

Digital appendices

1. Report text and figures (pdf)
2. Survey line maps (pdf and jpg)
3. NMO migrated sections (pdf)
4. NMO migrated sections (SEG-Y)
5. CMP coordinate files (xls)
6. Field coordinates (recording stations and shooting stations) (xls)
7. *SURPAC* files
    - 7.1 NMO migrated sections draped on CMP profiles
    - 7.2 Loops and strings digitized from the sections
        - Strong reflector boundaries (str)
        - Altered rocks at surface
            - Sericite-schist
            - Cordierite-antophyllite rock
        - Surface outcropt of the Pyhäsalmi ore deposit
        - Targets for further extrapolation
        - Surpac style files (ssi)
    - 7.3 Lithological map
    - 7.4 Airborne magnetic map